Magnetic Susceptibility in High Resolution NMR and MRI

Thomas M. Barbara

Oregon Health and Sciences University

A Note to Online Viewers of these Lecture Notes

These notes were created to accompany an actual real life lecture. Although I am sure I did not remember to state everything that I wanted to point out in the lecture , each slide was augmented by a dialogue that gave context. In essence, “ya shudda been there”. However, the online availability of the ENC tutorial sessions is a worthwhile pursuit and I trust that these notes will be useful even without the context of the lecture.

Some Resources

- J.H. Van Vleck, "*Electric and Magnetic Susceptibilities*".
- J.D. Jackson, "*Classical Electrodynamics*".
- Melvin Schwartz, "*Principles of Electrodynamics*".
- R.P. Feynman "Lectures on Physics".
- David Doty, G. Entzminger, Y. Yang, *Magnetism in High Resolution NMR Parts I & II. Concepts in Magnetic Resonance*.
- Dave Vander Hart, "*Magnetic Susceptibility in High Resolution NMR. Encyclopedia of Magnetic Resonance*".
- H.B.G. Casimir, "*Magnetism and Very Low Temperatures*".
- N.W. Ashcroft and N.D. Mermin, "*Solid State Physics*".
- C. Kittel, "*Introduction to Solid State Physics*".

Magnetostatics 101

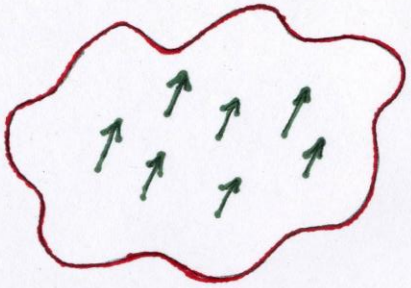

$$\underset{\sim}{H} = \underset{\sim}{B} - 4\pi \underset{\sim}{M}$$

$$\underset{\sim}{M} = \chi \underset{\sim}{H}$$

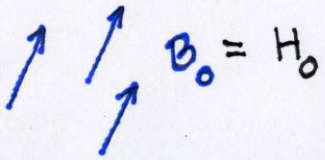

$\chi < 0$ Diamagnetic

$\chi > 0$ Paramagnetic

} Michael Faraday

$$\mu \underset{\sim}{H} = B = (1 + 4\pi\chi)^{-1} B \approx B(1 - 4\pi\chi)$$

Water $\chi_{dia} = -0.72$ ppm $\chi_{para} = 3 \times 10^{-4}$ ppm

$$B - B_0 = \delta B = \frac{4\pi}{3} B_0 \chi$$

M is the result of a collection of Magnetic Dipole Moments

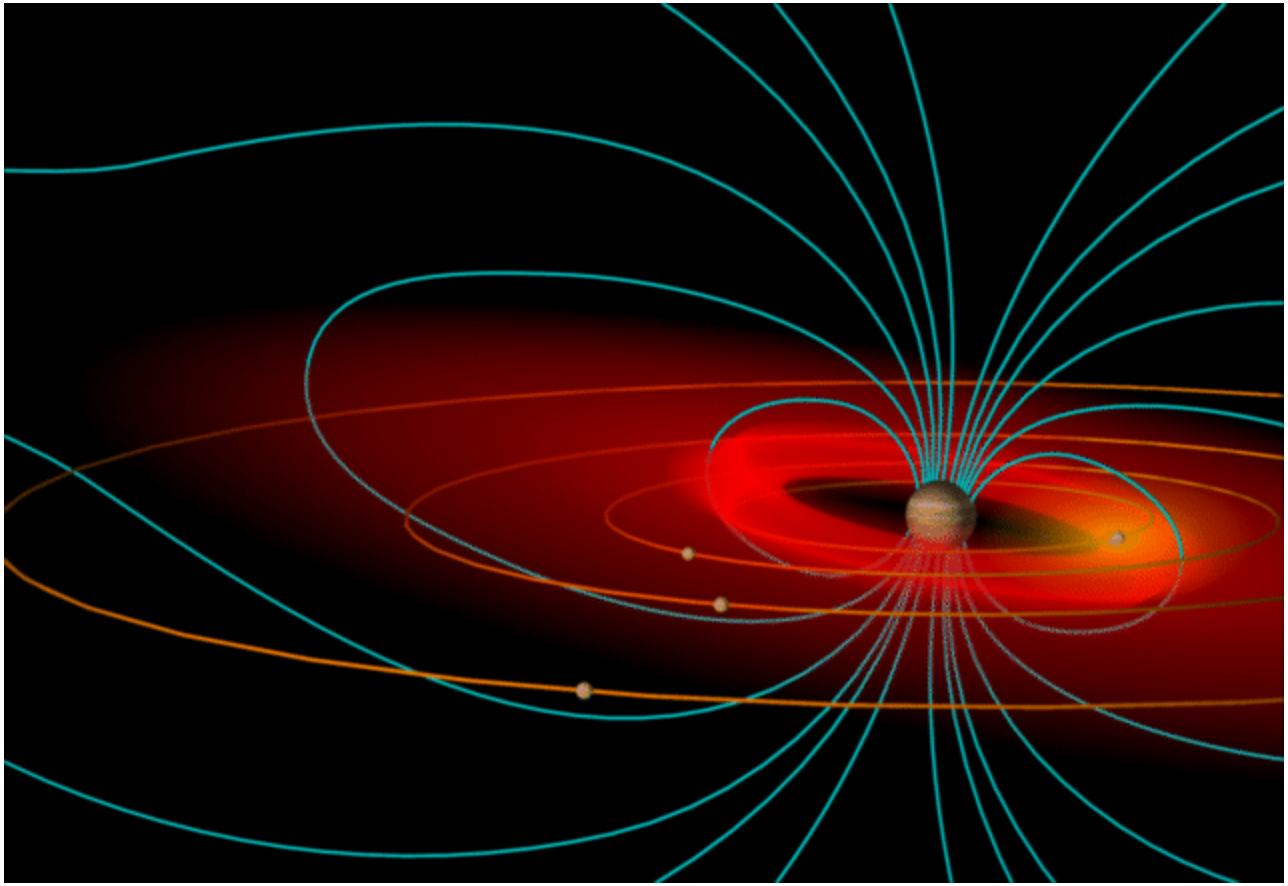

Some Philosophy Regarding B vs. H

It has been pointed out periodically that since $\bar{B}$ contains the induced magnetization as well as the direct effects of $\bar{H}$, it is the appropriate quantity to use in NMR of finite permability materials. We have taken the easy way out and used $\bar{H}$ throughout this book, however, simply because its use is nearly canonical in NMR and, despite the philosophical problems, therefore is unambiguous by usage. This is akin to a newly coined word in a language becoming an accepted word by usage, even though it never should have.

"Experimental Pulse NMR: A Nuts and Bolts Approach"
Fukushima and Roeder

At this point we must interject a small bit of philosophy. It is customary to call **B** the magnetic induction and **H** the magnetic field strength. We reject this custom inasmuch as **B** is the truly fundamental field and **H** is a subsidiary artifact. We shall call **B** the magnetic field and leave the reader to deal with **H** as he pleases.

"Principles of Electrodynamics"
Melvin Schwartz

As we will see later, there is a **physical** reason why one can use either field in NMR


Miss van Leeuwen, you are Magnetic!
Oh, Niels... Only in a QUANTUM WORLD!
Ψ^+ or Ψ^- ?

Quantum Origins of Magnetism

Classical Theory Predicts Zero Magnetic Effects
(Bohr - van Leeuwen Theorem)

- Intrinsic Moments (Currents) of Particles
  M=C(B/T) Curie Langevin
- Induced Electronic Currents in Atoms and Molecules
- Chemical Shift and Molecular Susceptibility
- Landau Diamagnetism and Pauli Para-magnetism in Metals

Magnetic Shielding and Susceptibility Anisotropies

BERNARD R. APPLEMAN AND
BENJAMIN P. DAILEY

DEPARTMENT OF CHEMISTRY, COLUMBIA UNIVERSITY, NEW YORK, NEW YORK

I. Introduction

The last several years have seen significant advances in both experimental and theoretical techniques for the study of magnetic shielding and magnetic susceptibility. These advances have served not only to expand these areas but have also tended to develop a more complementary relationship and greater interdependence between the sometimes distant theoretical and experimental wings, particularly for shielding. Among the most important elements of this new relationship are the following: (a) a wider adoption of absolute shielding scales; (b) the increased use of *ab initio* calculations for shielding tensors of second period atoms; (c) the development of better experimental techniques for measuring chemical shifts of rare nuclei such as C-13 and N-15; (d) the development of methods which provide more complete information about the chemical shielding tensors.

There is a very close Connection between Chemical shift and Magnetic susceptibility.

Susceptibility Matching

- Eliminate magnetic perturbations from the NMR sample vicinity.
- NMR Coil and Sample
- Increasing challenges as Magnetic Fields increase (1 GHz).
- Background Signals
- Maintain Sensitivity

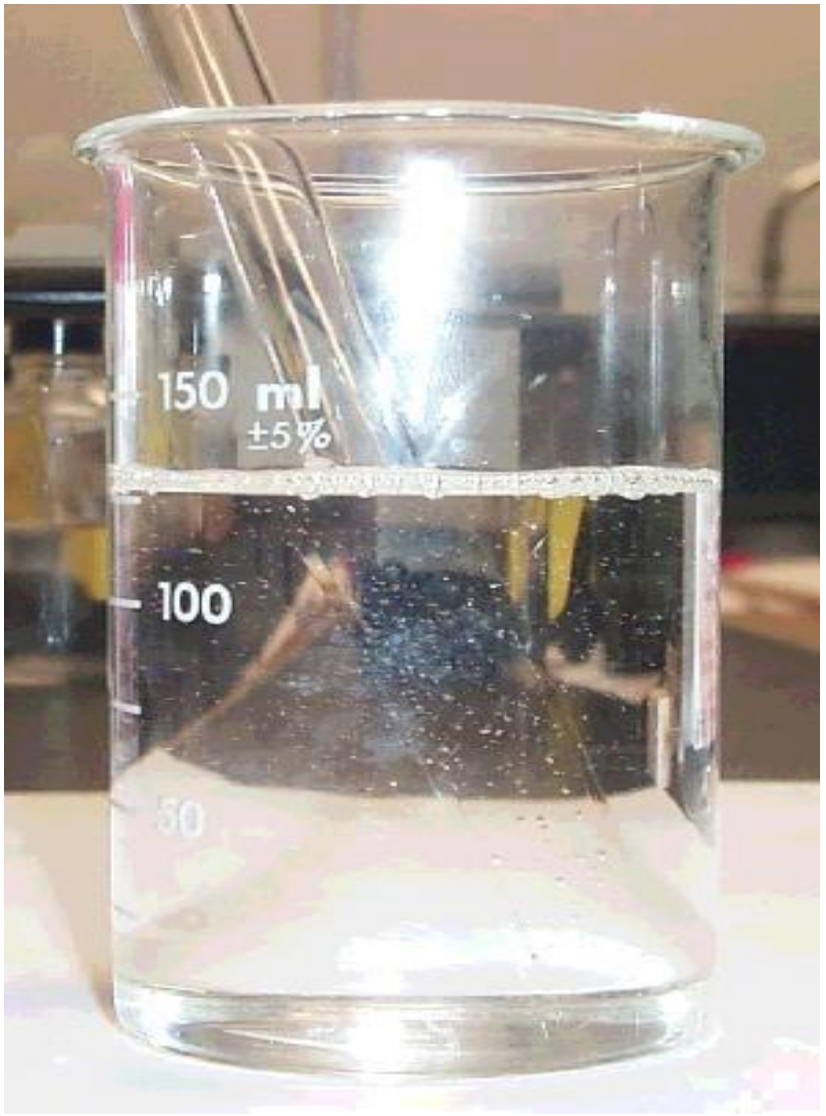

Matching susceptibilities is similar to matching the index of refraction.

ON THE PRINCIPAL MAGNETIC SUSCEPTIBILITIES OF CRYSTALS

By I. I. Rabi

Abstract

A new method of measuring the principal magnetic susceptibilities of crystals.—The crystal to be measured is immersed in a solution, the susceptibility of which is varied, and the orientation of the crystal adjusted till there is no movement of the crystal due to the magnetic field. The susceptibilities of the solutions are then measured. From these values the principal susceptibilities can then be easily obtained. The method does not require any preparation of crystal sections, measurement of the magnetic field or gradient of the field. The range of application of this method is for volume susceptibilities of -0.9×10^{-6} to $+70\times10^{-6}$.

The principal magnetic susceptibilities of certain crystals.—The above method is applied to the measurement of principal susceptibilities of 14 crystals. Of these eleven are paramagnetic, and belong to the monoclinic double sulphate hexahydrate isomorphous series, $MeSO_4 \cdot R_2SO_4 \cdot 6H_2O$. With these crystals the results seem to indicate that, unlike the optical and crystallographic properties, the principal susceptibilities and their relative magnitudes depend almost entirely on the paramagnetic ion alone. The influence of the alkali or ammonium ion is secondary. In the series containing copper the greatest difference in maximum and minimum susceptibilities is 28% of the average susceptibility, in the nickel series 4%, in the Co series 32%, in the Fe series 16% and in the Mn series 1%. Of the diamagnetic crystals, $NaNO_3$ and KNO_3, which are similar in their crystallographic properties to calcite and aragonite respectively, show similar magnetic properties.

NMR Sample Plugs

Shigemi Tube : Matched to Water

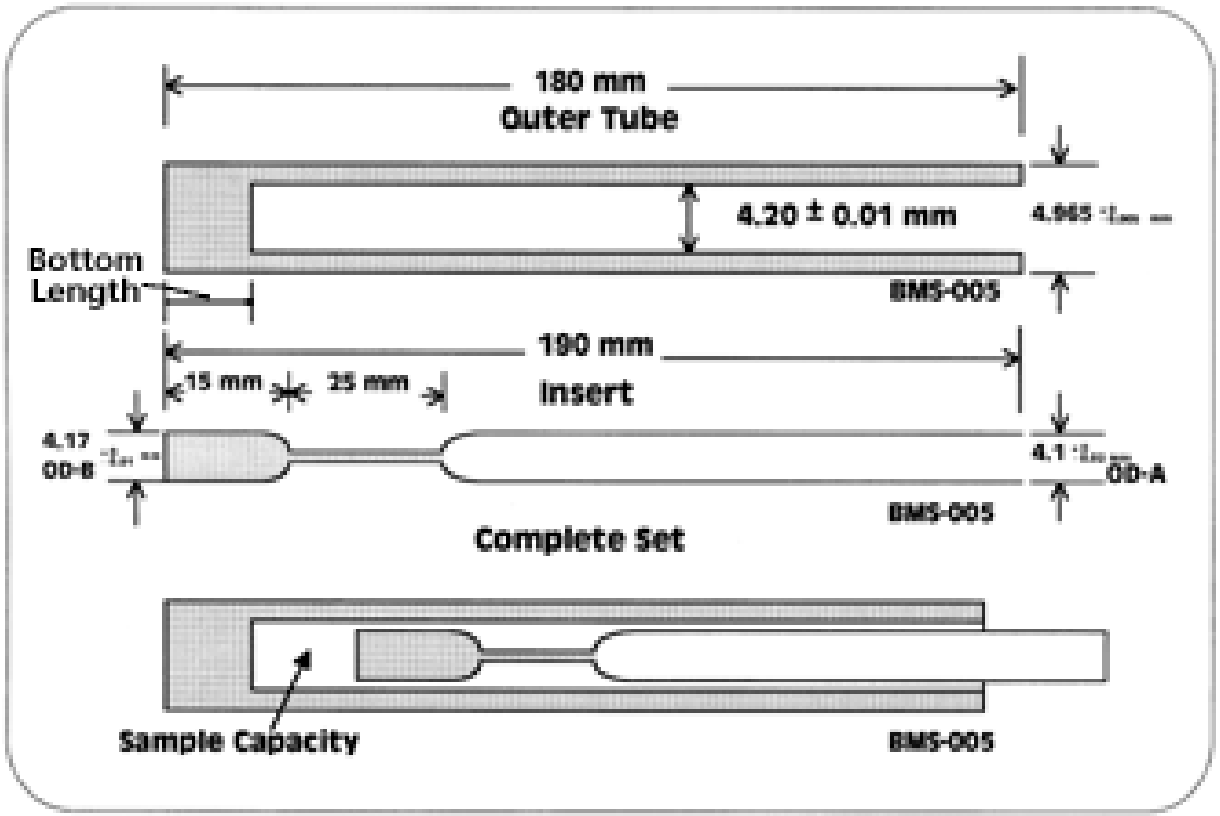

FC-43 as plugs in 3 mm NMR tubes
H.C. Jarrell JMR 198, 204 (2009)

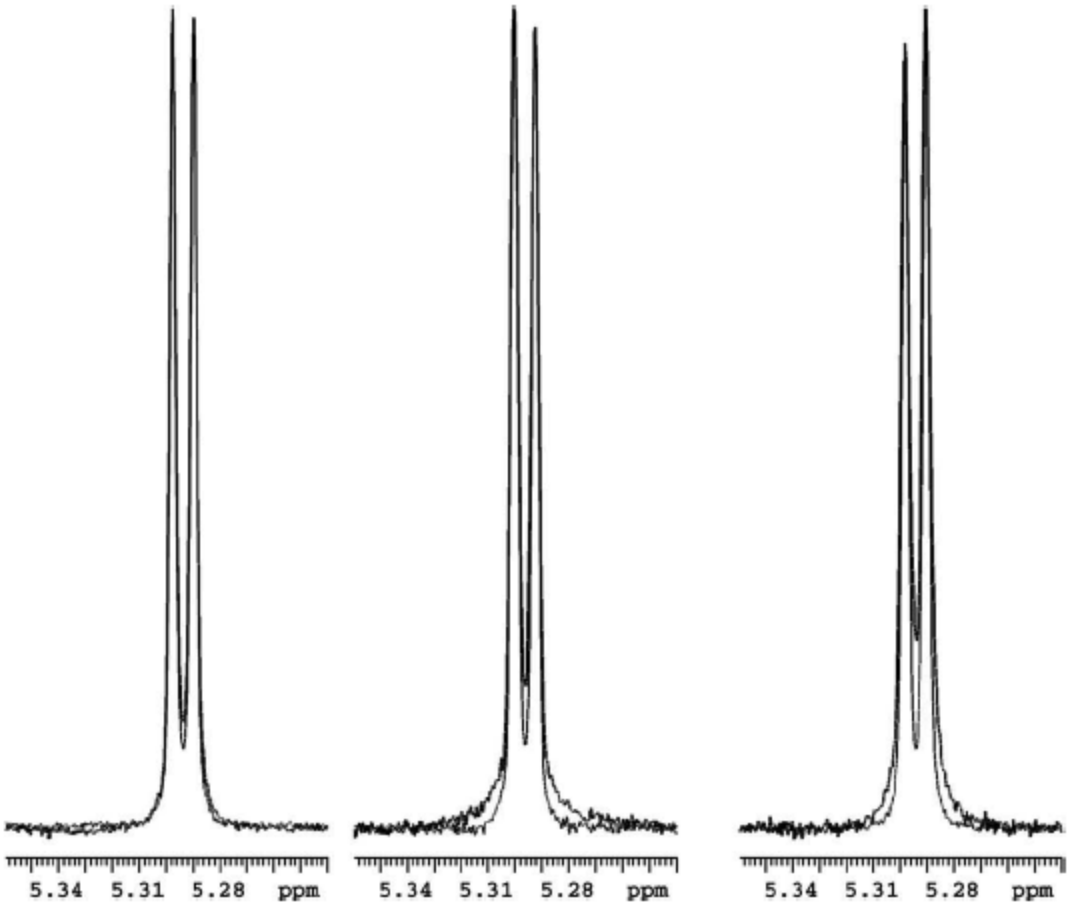

Fig. 1. Comparison of 500 MHz ^{1}H NMR spectra of 1.9 mM sucrose in D_2O acquired with 180 µl standard (thin line) sample and (thick line) confined between two 80 µl volumes of FC-43 in 3 mm (o.d.) NMR tubes. (A) 65 µl at 25 °C. (B) 65 µl at 60 °C and (C) 40 µl at 25 °C. Samples were gradient shimmed with the same shim map except at 60 °C. Spectra were acquired with identical conditions, on an INOVA 500 spectrometer and a 3 mm probe with water presaturation and processed with identical parameters. No line broadening was used in the processing.

PdCu Reel to Reel Wire

25 mil Thomas M. Barbara 2/5/02

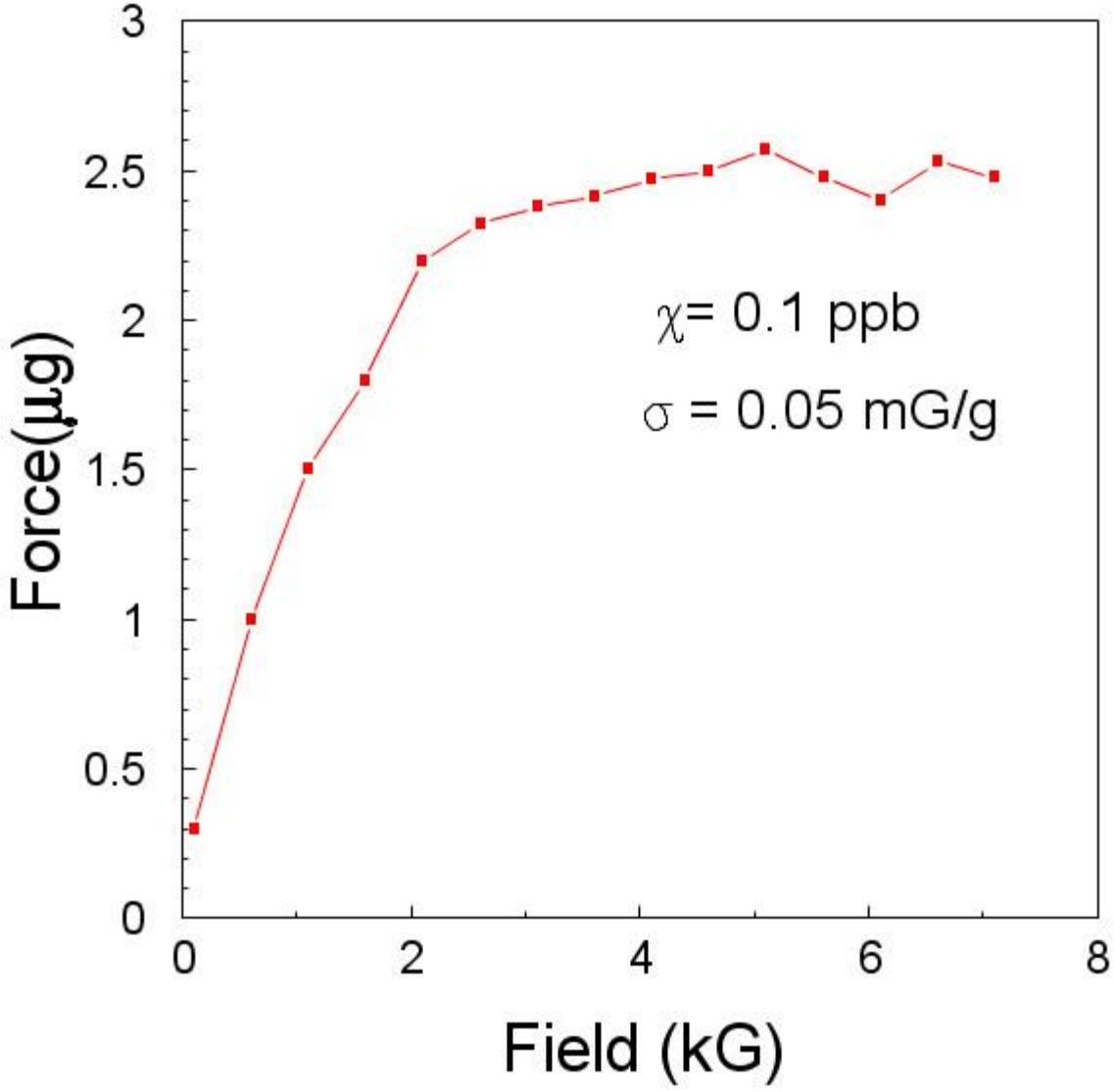

PdCu Sample in N_2 and Air

4 mil material T.M. Barbara 5/14/97

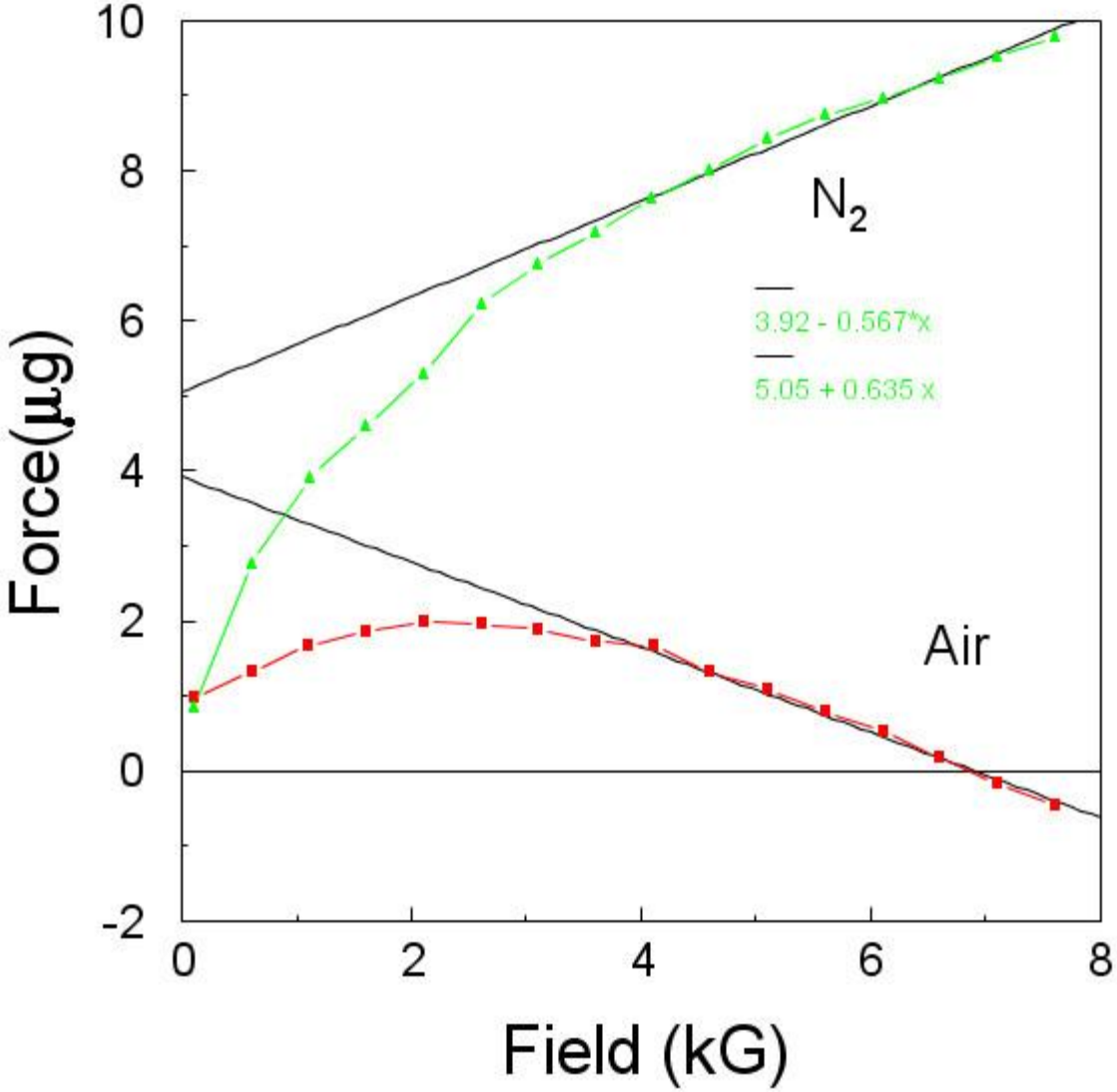

US005684401A

United States Patent [19]

Peck et al.

[11] Patent Number: 5,684,401

[45] Date of Patent: Nov. 4, 1997

[54] **APPARATUS AND METHOD FOR COMPENSATION OF MAGNETIC SUSCEPTIBILITY VARIATION IN NMR MICROSPECTROSCOPY DETECTION MICROCOILS**

[75] Inventors: **Timothy L. Peck**; **Dean L. Olson**, both of Champaign; **Jonathan V. Sweedler**, Urbana; **Andrew G. Webb**, Urbana; **Richard L. Magin**, Urbana, all of Ill.

[73] Assignee: **Board of Trustees of the University of Illinois**, Urbana, Ill.

[21] Appl. No.: **595,269**

[22] Filed: **Feb. 1, 1996**

[51] **Int. Cl.**[6] **G01V 3/00**

[52] **U.S. Cl.** **324/318**; 324/321

[58] **Field of Search** 324/300, 307, 324/309, 312, 314, 306, 318, 321, 322

[56] **References Cited**

U.S. PATENT DOCUMENTS

5,394,088	2/1995	Cory	324/322
5,416,414	5/1995	Mansfield et al.	324/321

OTHER PUBLICATIONS

Bhagwandien, R. et al. "Numerical Analysis of the Magetic Field for Arbitrary Magnetic Susceptibility Distributions in 2D", *Magnetic Resonance Imaging*, Vol. 10, 1992, pp. 299–313.

Odeblad, Erik, "Miro–NMR in High Permanent Magnetic Fields", Acta Obstetricia et Gynecologica Scandinavica, vol. XLV, Supplement 2, 1966, pp. 84–119.

Albert, K., "On–Line Use of NMR Detection in Separation Chemistry", *Journal of Chromatography*, 703, 1995, pp. 123–147.

Apte, D.V. et al., "Phosphorus–31 NMR Spectroscopic Studies of Single Living Toad Retina", Abstracts, Society of Magnetic Resonance in Medicine, San Francisco, CA, Aug. 1988.

Black, R.D. et al., "A High–Temperature Superconducting Receiver for Nuclear Magnetic Resonance Microscopy", *Science*, Feb. 5, 1993, vol. 259, pp, 683–795.

Black, R.D. et al., "Performance of a High–Temperature Superconducting Resonator for High–Field Imaging", *Journal of Magnetic Resonance*, Series A 113, 1995, pp. 74–89.

Cho, Z.H. et al. "Nuclear Magnetic Resonance Microscopy with 4–μm resolution; Theoretical Study and Experimental Results", *Med. Phys.*, Nov./Dec. 1988, 15 (6), pp. 815–824.

Chu, Simon C.K. et al, "Bulk Magnetic Susceptibility Shifts in NMR Studies of Compartmentalized Samples: Use of Paramagnetic Reagents", *Magnetic Resonance in Medicine*, 1990, 13, pp. 239–262.

Fuks, L.F. et al., "Susceptibility, Lineshape, and Shimming in High–Resolution NMR", Journal of Magnetic Resonance, 100, 1992, pp. 229–242.

Lemarquard, G. et al., "Annular Magnetic Position Sensor." *IEEE Transactions on Magnetics*, vol. 26, No. 5. Sep. 1990.

(List continued on next page.)

Primary Examiner—Louis M. Arana
Attorney, Agent, or Firm—Woodard, Emhardt, Naughton Moriarty & McNett

[57] **ABSTRACT**

An apparatus and method for compensation of magnetic susceptibility variation in NMR microspectroscopy detection microcoils. NMR detection microcoils are formed with side-by-side windings in order to approximate a uniform cylindrical sheet coil. The wire may have a thin layer of insulation in order to prevent shorting between adjacent turns, or (if the wire diameter is small enough) uninsulated wire may be wound with the adjacent turns touching without fear of shorting between coil turns. Additionally, a susceptibility matching medium, such as a perfluorinated hydrocarbon, may be placed around the microcoil to minimize susceptibility-induced variations in the B_0 magnetic field.

15 Claims, 4 Drawing Sheets

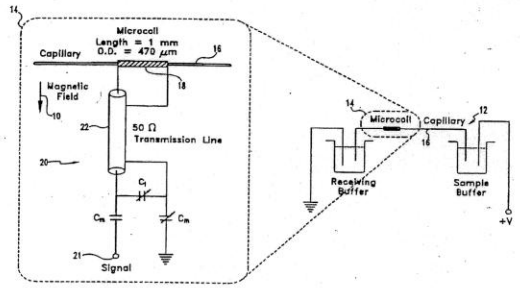

US005545994A

United States Patent [19]

Barbara

[11] Patent Number: 5,545,994

[45] Date of Patent: Aug. 13, 1996

[54] **REDUCTION OF AMBIENT SUSCEPTIBILITY PERTURBATIONS OF AN NMR SPECTROMETER**

[75] Inventor: **Thomas M. Barbara**, Cupertino, Calif.

[73] Assignee: **Varian Associates, Inc.**, Palo Alto, Calif.

[21] Appl. No.: **433,637**

[22] Filed: **May 2, 1995**

[51] **Int. Cl.**[6] **G01V 3/00**

[52] **U.S. Cl.** **324/315**; 324/321

[58] **Field of Search** 324/315, 317, 324/321, 318, 306, 307, 309

[56] **References Cited**

U.S. PATENT DOCUMENTS

3,091,732	5/1963	Anderson et al.	324/0.5
4,266,194	5/1981	Hlavka	324/315
4,461,996	7/1984	Kwon	324/315
5,096,826	3/1992	Barbic et al.	324/317

Primary Examiner—Louis M. Arana
Attorney, Agent, or Firm—Edward Berkowitz

[57] **ABSTRACT**

The volume magnetic susceptibility of an NMR probe is established and maintained at a desired value, such as a value characterizing other components of the probe, by a linear combination of partial pressures of respective fluids introduced into the sensitive volume of the probe.

5 Claims, 5 Drawing Sheets

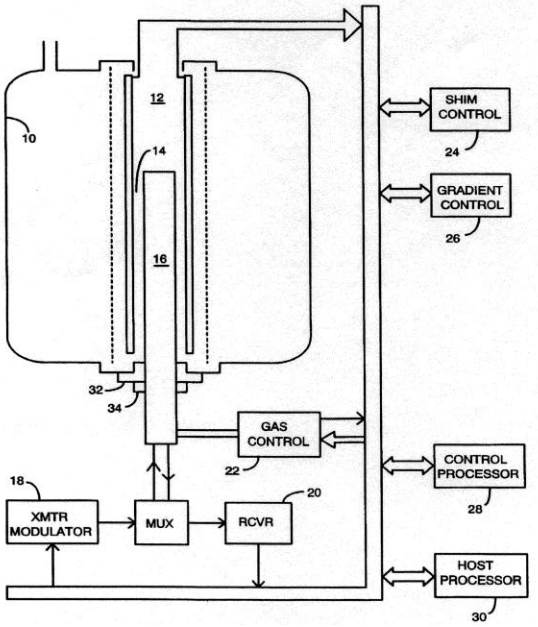

600 MHz Lineshape "Air Shimmed" VS Nitrogen

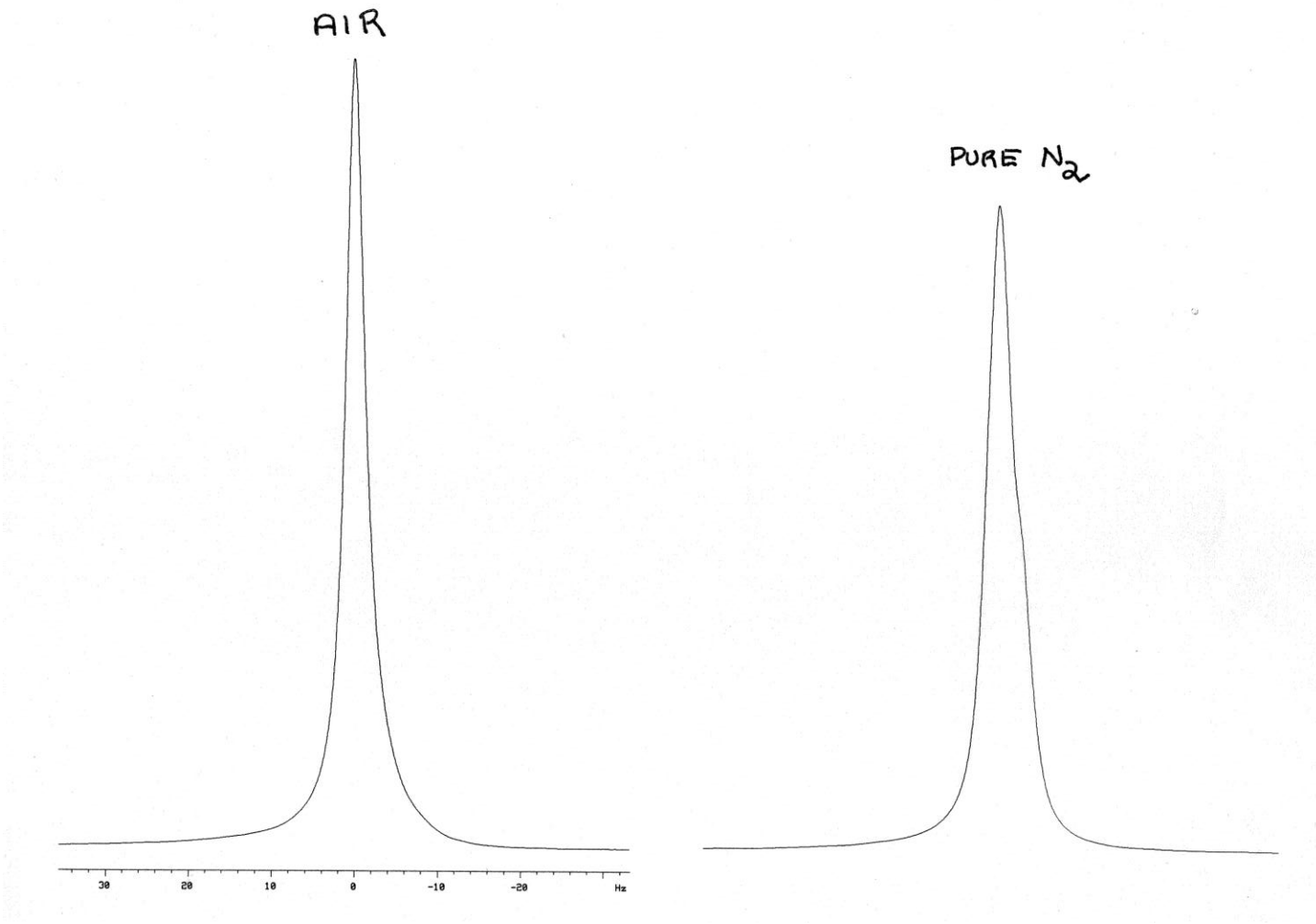

Alderman-Grant Resonator

Composed of a tri-layer foil
M1-M2-M1

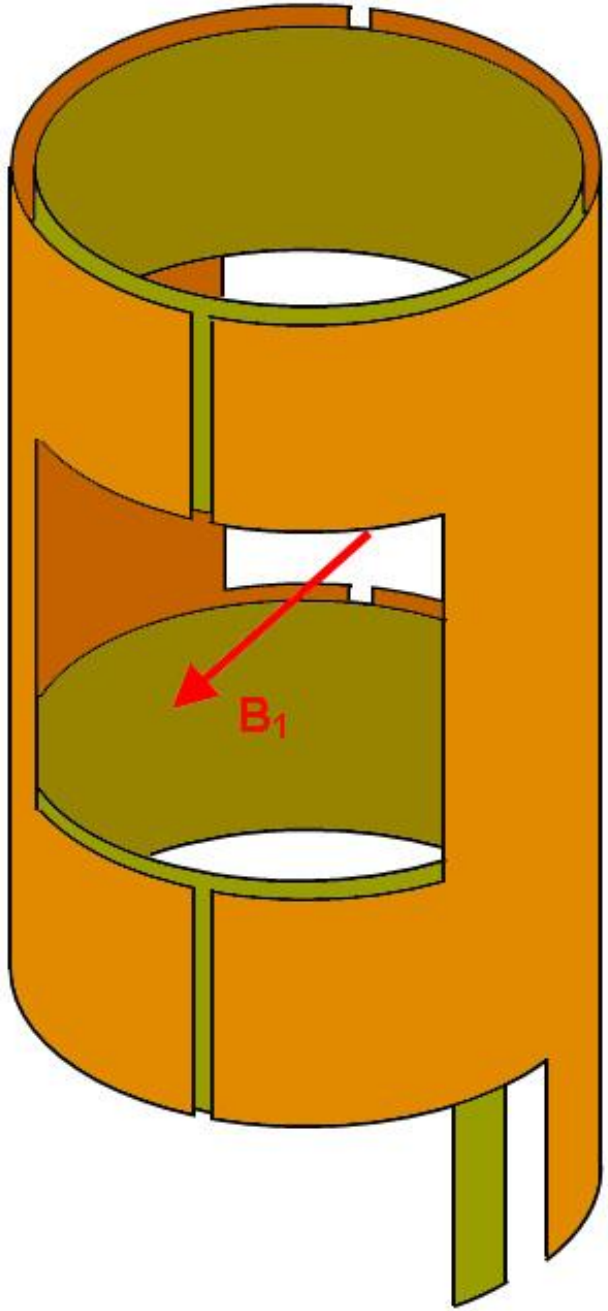

600 MHz Lineshape VS Layer Matching

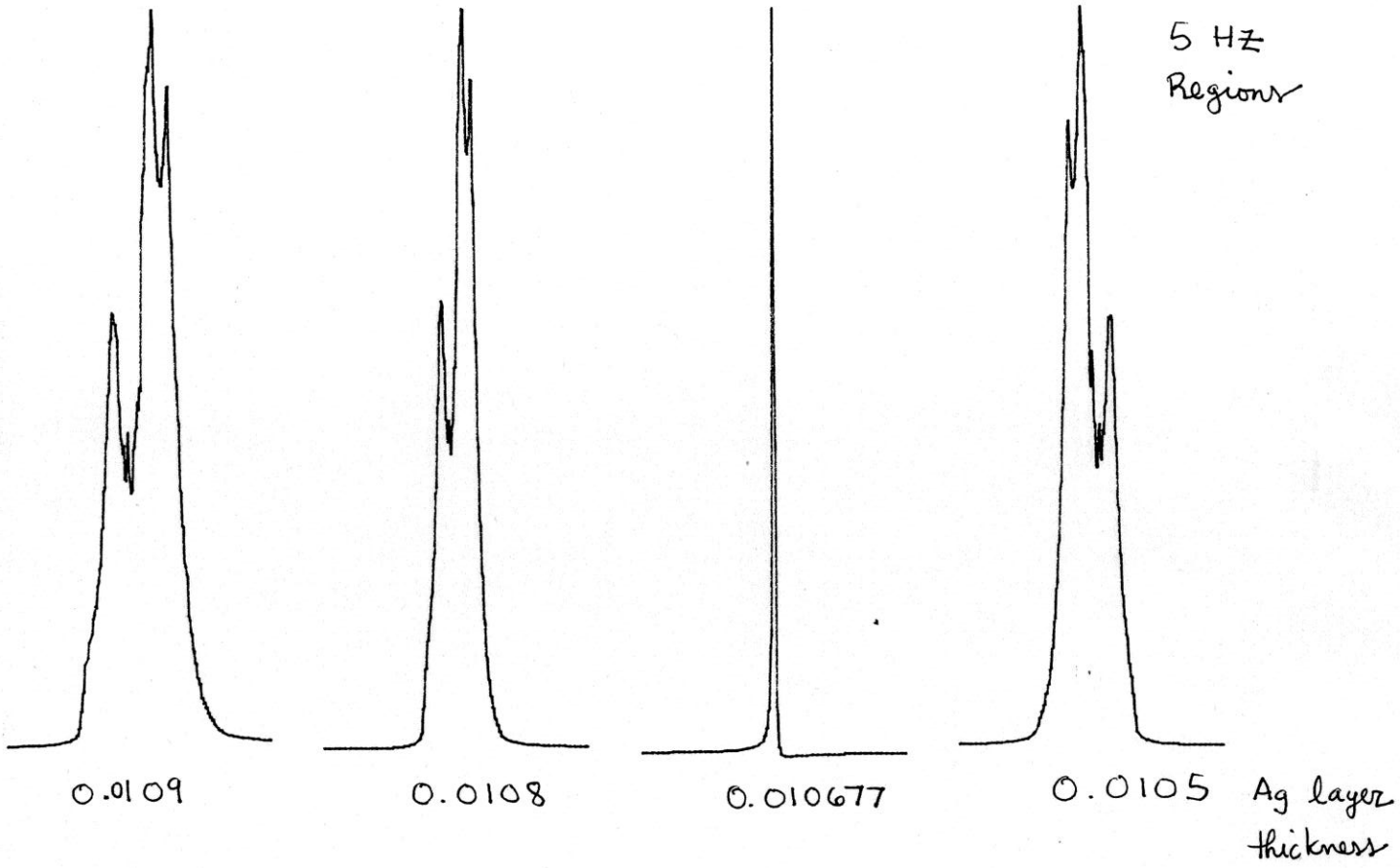

Fine Structure at “Exact Match”

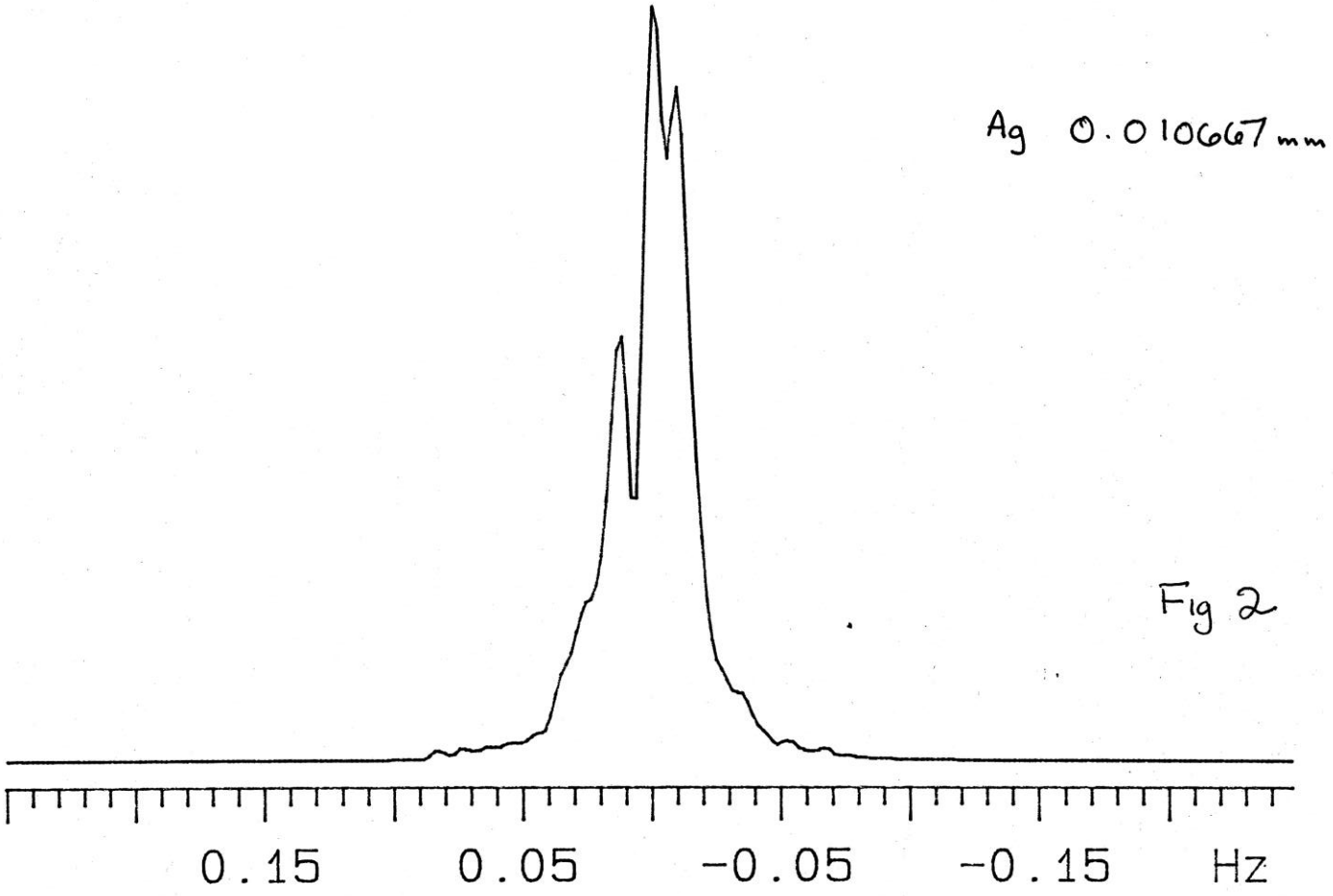

Magnetic Field Dynamics in MR systems
N. De Zanche et. al. MRM 60,176 (2008)

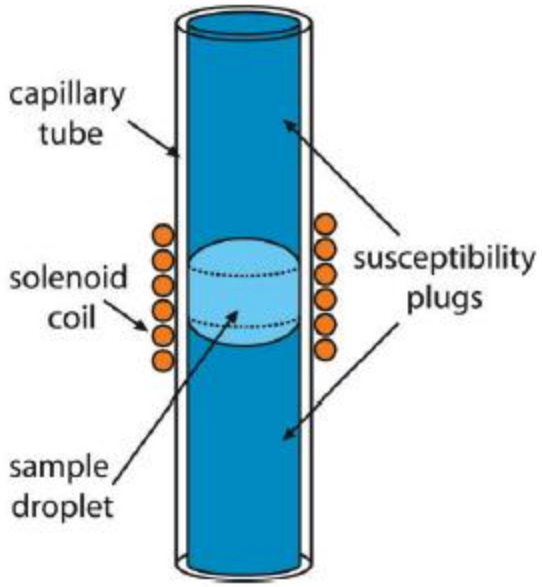

FIG. 1. NMR probehead consisting of a sample droplet suspended between liquid susceptibility plugs within a capillary, inserted into a solenoid detector coil.

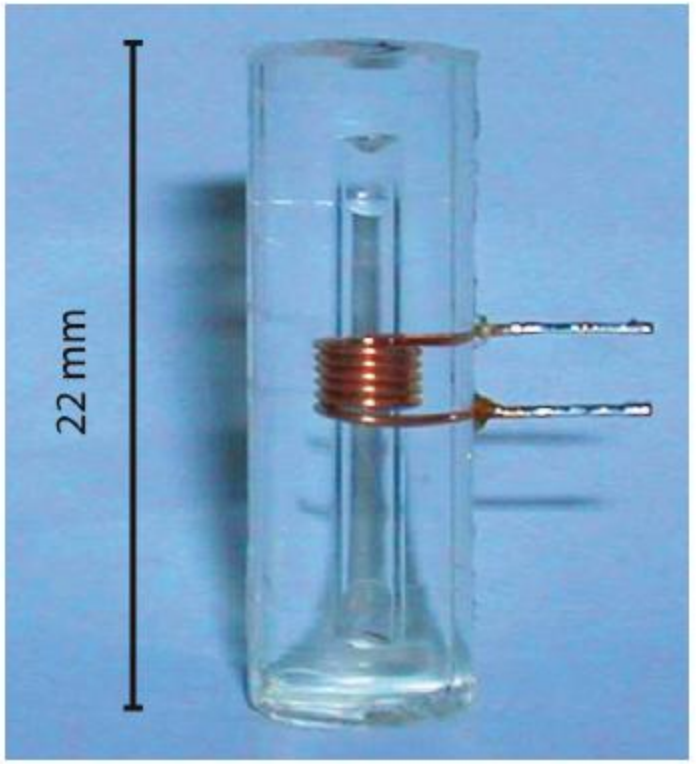

FIG. 2. Probehead based on a cyclohexane droplet with doped D_2O plugs and epoxy casing. The signal-to-noise ratio (SNR) yield of this design is on the order of $2 \times 10^5 \sqrt{\text{Hz}}$. For instance, at a sampling rate of 100 kHz its initial SNR is approximately 630.

P. Sipila et. al. Sensors and Actuators A145, 139 (2008)

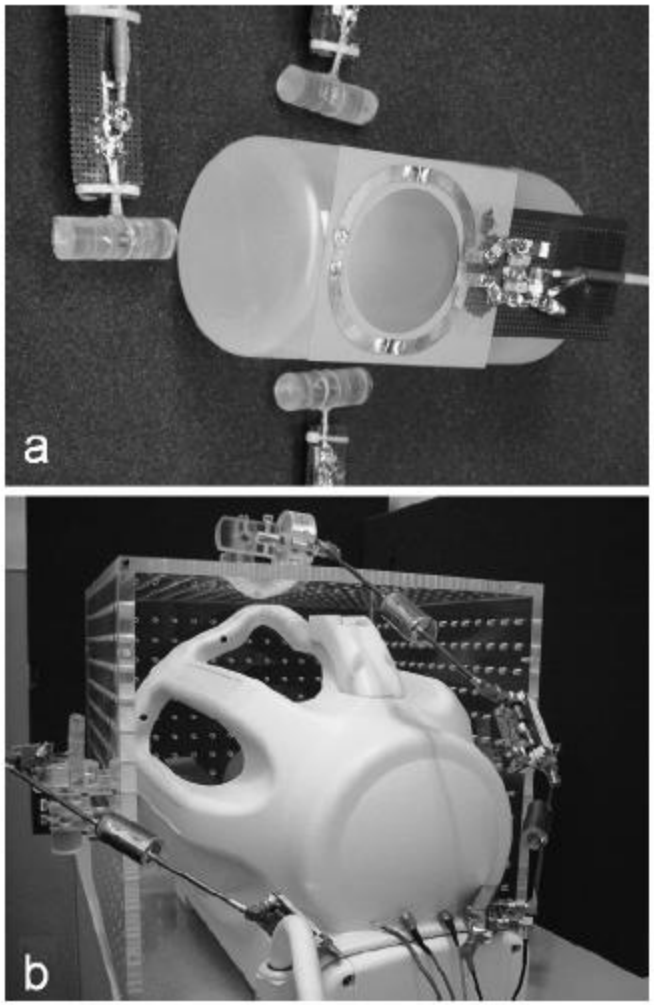

Fig. 5. Experimental setups for acquiring an image with a single surface coil (a) and with an 8-channel head coil (b). The image acquisition was assisted by three field monitoring NMR probes.

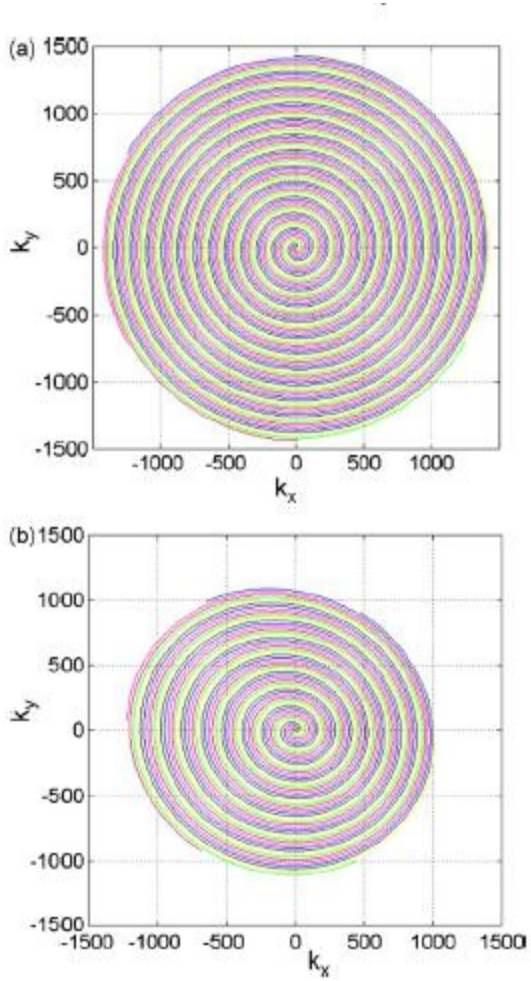

Fig. 8. Multi-shot spiral imaging trajectories of the Fig. 7. The picture on left (a) shows the ideal and the right (b) the measured trajectory.

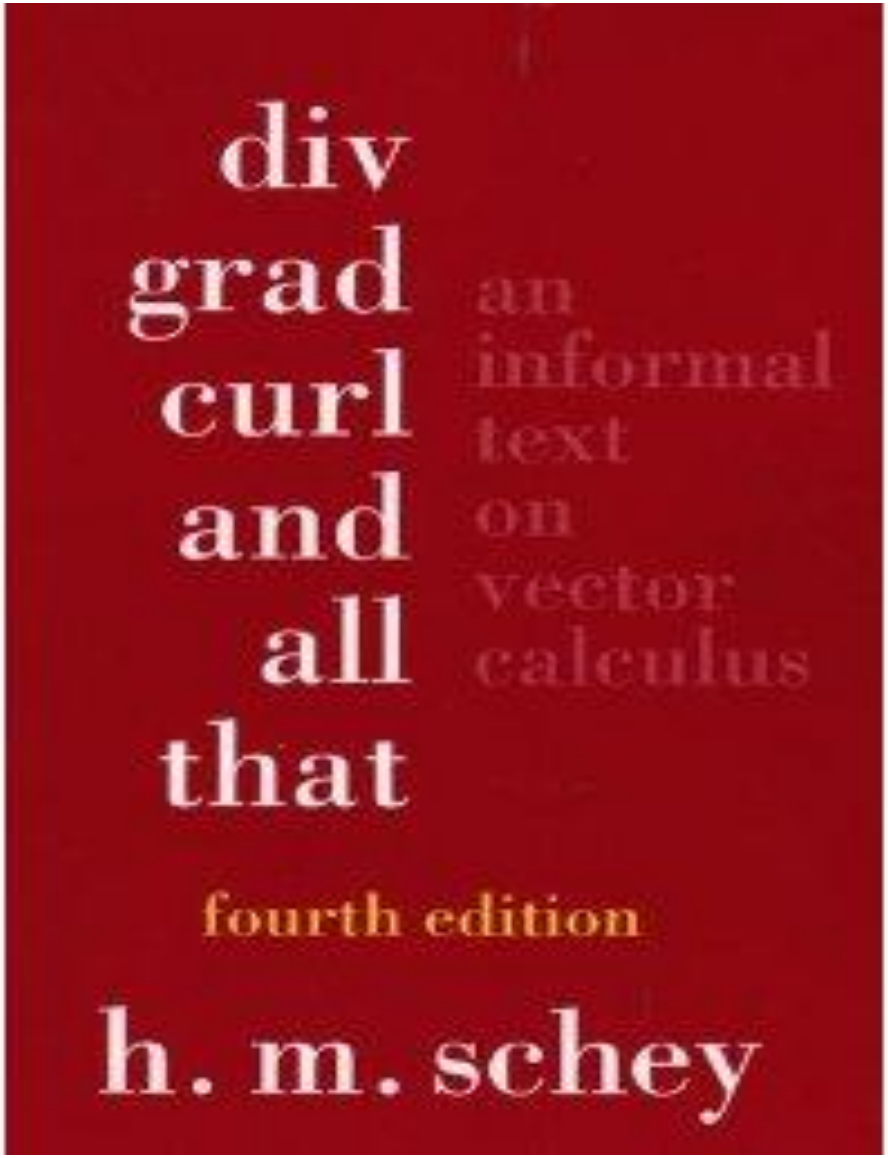

Yes, More Theory is Coming Up!

Equivalent "Currents" and "Charge"

$$\underset{\sim}{J} = \underset{\sim}{\nabla} \times \underset{\sim}{M} \qquad \rho = -\underset{\sim}{\nabla} \cdot \underset{\sim}{M}$$

$$\underset{\sim}{K} = \underset{\sim}{n} \times (\underset{\sim}{M}_2 - \underset{\sim}{M}_1) \qquad \sigma = -\underset{\sim}{n} \cdot (\underset{\sim}{M}_2 - \underset{\sim}{M}_1)$$

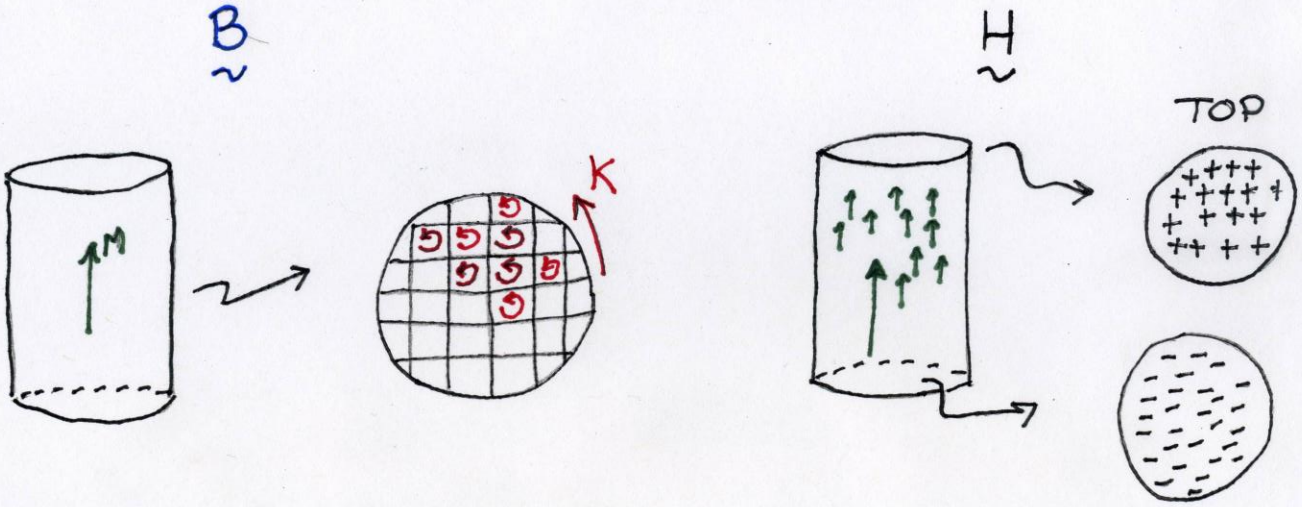

Summation of Dipoles
Can be Inefficient

Equivalent Currents

$$\underset{\sim}{J} = \underset{\sim}{M} \times \underset{\sim}{n}$$

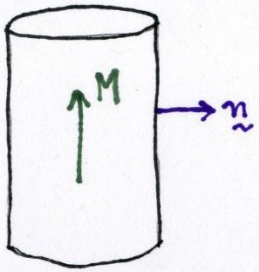

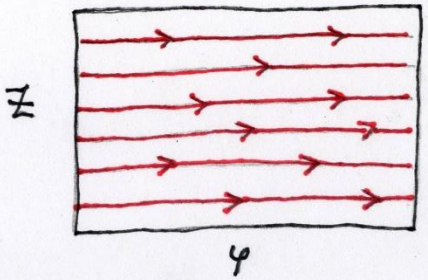

SOLENOID

$J_\varphi = \text{Const}$

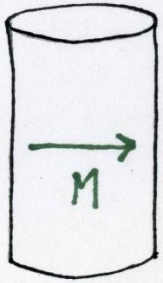

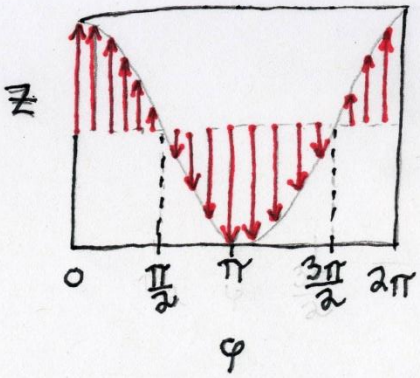

BIRDCAGE

$J_z = \cos\varphi$

Thinking about magnetized cylinders is similar to thinking about RF Coils!

The Cylinder

(aka The NMR tube)

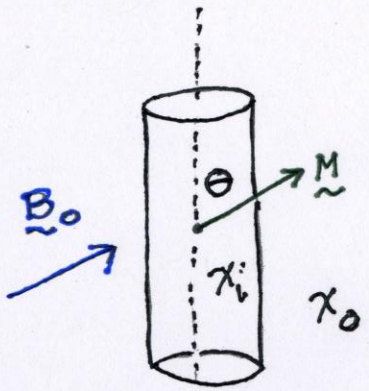

$$\underset{\sim}{K} = (\underset{\sim}{M}_{in} - \underset{\sim}{M}_{out}) \times \underset{\sim}{n}$$

$$|\underset{\sim}{K}| = (\chi_i - \chi_0) B_0$$

$$\delta\underset{\sim}{B} = \underset{\sim}{B}_{in} - \underset{\sim}{B}_0 = (\chi_i - \chi_0) B_0 \{ 4\pi \cos\theta \, \underset{\sim}{e}_z - 2\pi \sin\theta \, \underset{\sim}{e}_y \}$$

$$\delta\underset{\sim}{H} = \delta\underset{\sim}{B}_{in} - 4\pi \underset{\sim}{M}$$

$$= -2\pi (\chi_i - \chi_0) B_0 \sin\theta \, \underset{\sim}{e}_y$$

Hmmm . . . This does NOT Look Very "Philosophical"

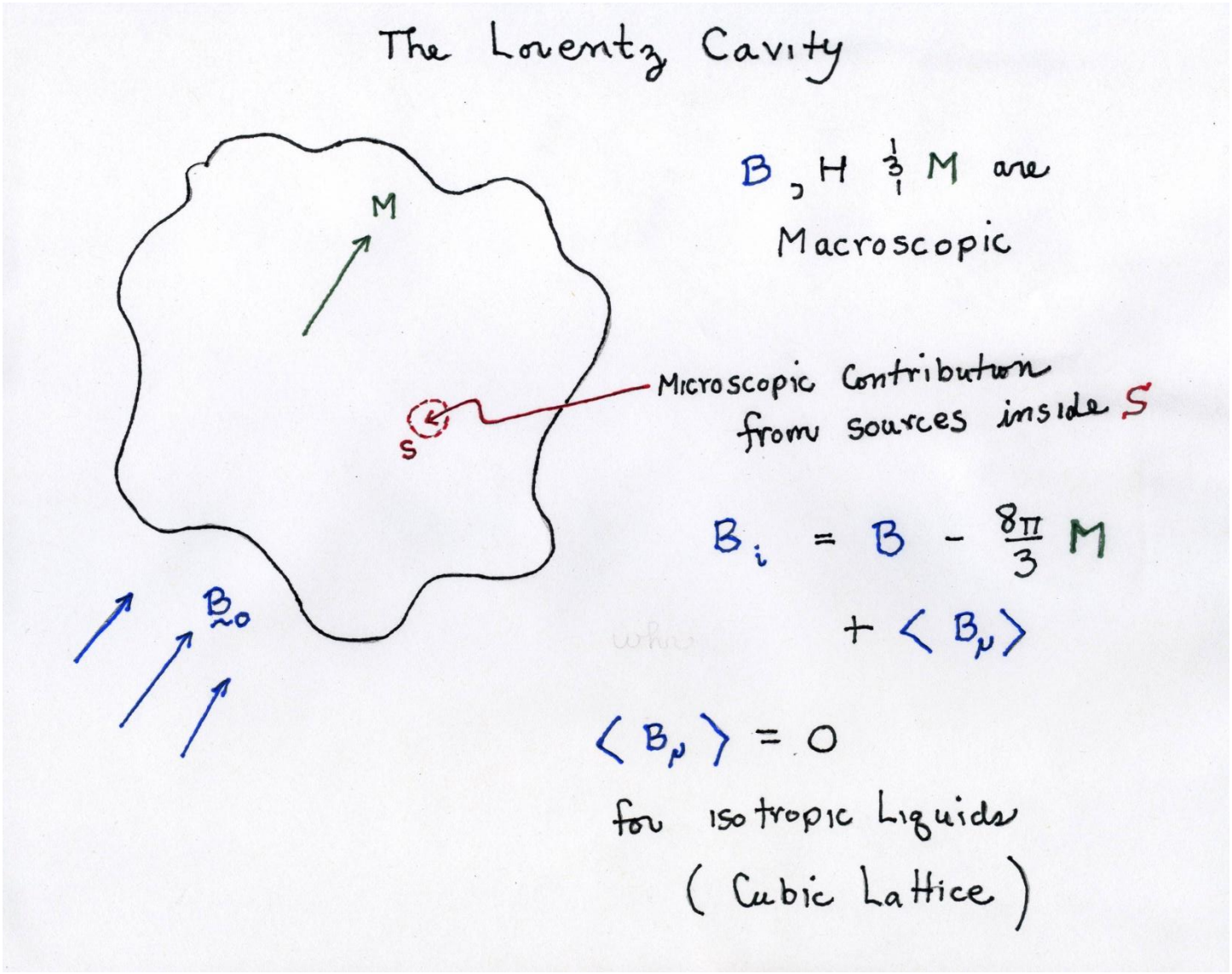

The Lorentz Cavity is constructed to separate long range from short range contributions. For isotropic environments the short range effects average to zero.

NESTED BOUNDARIES

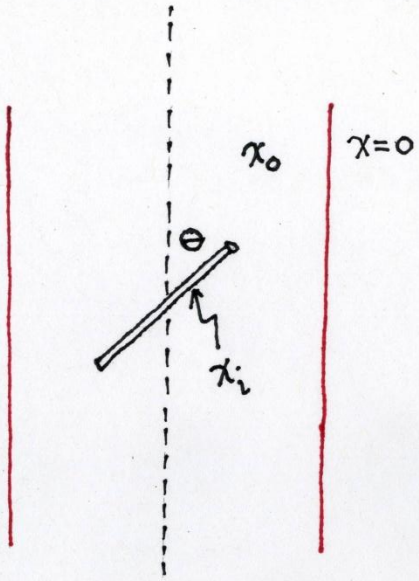

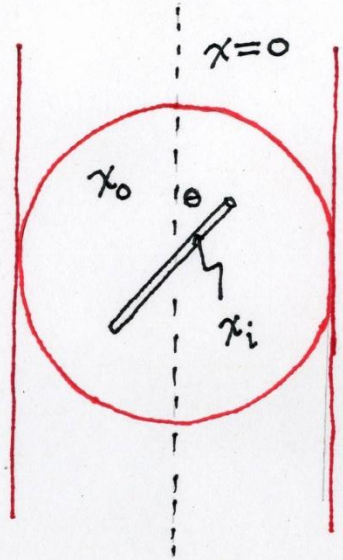

$\delta B/B_0 = \delta H/H_0$

$\frac{4\pi}{3}\left[(\chi_i-\chi_0)P_2(\cos\theta)+\chi_0\right]$

$\delta B/B_0 = \delta H/H_0$

$\frac{4\pi}{3}(\chi_i-\chi_0)P_2(\cos\theta)$

$$H + \frac{4\pi}{3}M = B - \frac{8\pi}{3}M$$

Proper treatment of boundaries : Consider all surfaces !

The **B Field** VS the **H Field** in NMR

The simple calculation above illustrates that as a result of the Lorentz cavity correction, one can use either B or H in NMR . If one uses B, then the Lorentz correction is $-8\pi/3$. If one uses H, the correction is $+4\pi/3$.

In the older literature, the use of H, with the correct correction, was prevalent. More recently, the B field was adopted. It could very well be, that one used H and meant B, or B and meant H. **One can find out what they really meant** by looking at the Lorentz correction, if one was used. If one was not, then the assumption was the spins were in a vacuum and of course in that case B=H.

C. Boesch et. al. MRM 37,484 (97)
S.K. Chu et. al. MRM 13,239 (90)

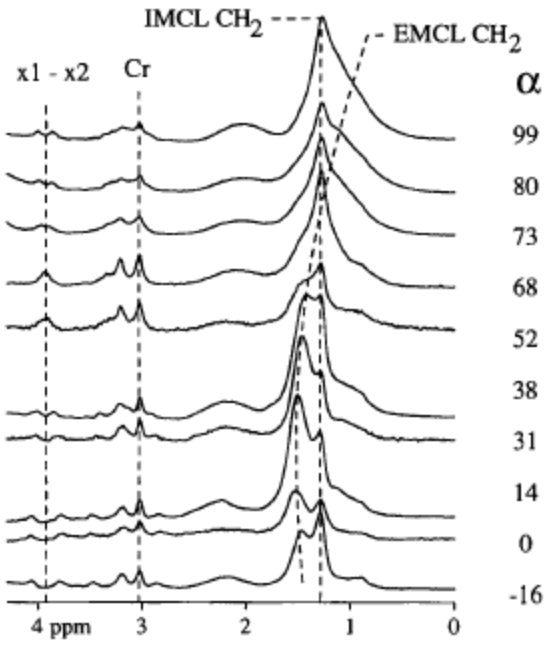

FIG. 4. Series of ^{1}H-MR spectra of *M. tibialis anterior* in a 32 y old female volunteer with her calf at different angles with respect to the static magnetic field. Chemical shift reference is the CH_3-signal of Cr at 3.02 ppm. While one part of the lipid CH_2 signals at 1.25 ppm is constantly visible at all different angles, a second portion of signals shows a variable resonance frequency as well as an angle-dependent broadening of the signal (broken line for illustration only). The amount of the shifting resonance (EMCL) varies considerably since the voxel is aligned along the main axes of the magnet. Best separation between the two signals is achieved when the tibialis muscle is roughly parallel to the static magnetic field. This is consistent with theory (see Appendix). The variable splitting of the X1-X2 doublet is due to dipolar coupling of the CH_2 protons of creatine and is described and analyzed in (17, 18).

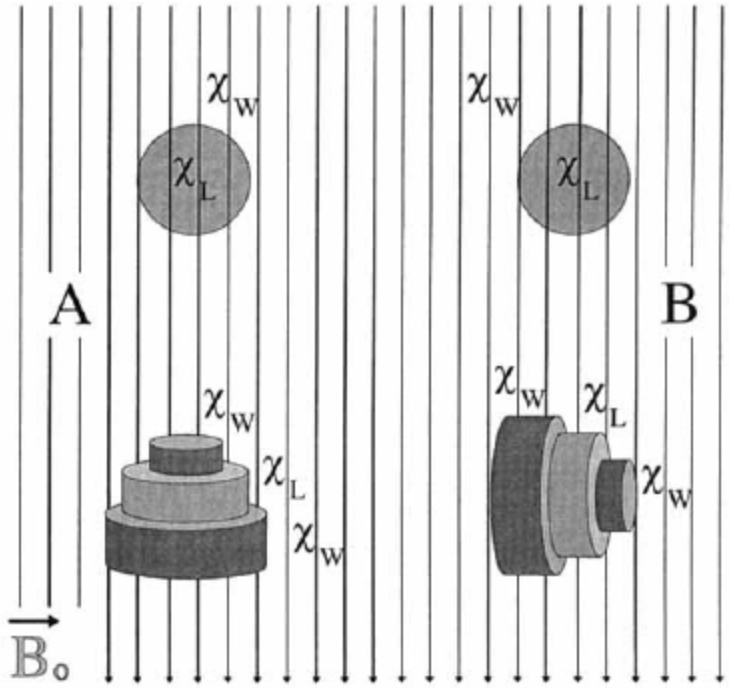

FIG. 11. Comparison of susceptibility effects on spherical and tubular structures at two different angles with respect to the static magnetic field B_0. The left side (A) illustrates the case where muscular fibers are parallel to B_0 (i.e., vertical); the right side (B) shows muscular fibers perpendicular to B_0. While susceptibility effects acting on spherical structures (such as lipid droplets) are independent of the angle between muscle fiber and B_o, tubular structures are subject to anisotropic susceptibility shifts, as described in the Appendix.

The Cylinder (Exterior Solution)

$$\underset{\sim}{B}_{OUT} = 2\pi \Delta\chi \sin\theta \left(\frac{a^2}{\rho^2}\right)\left(\sin 2\varphi \, \underset{\sim}{e}_x - \cos 2\varphi \, \underset{\sim}{e}_y\right)$$

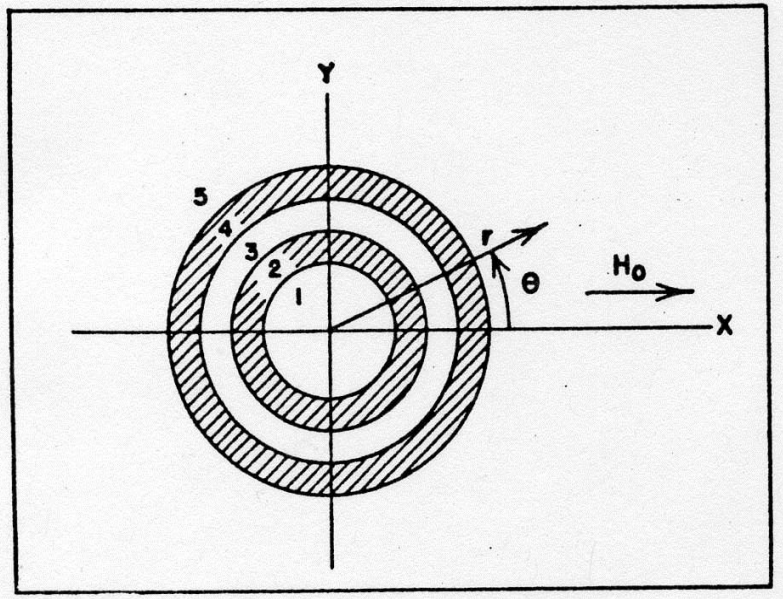

Fig. 5.—Coaxial system for standardization.

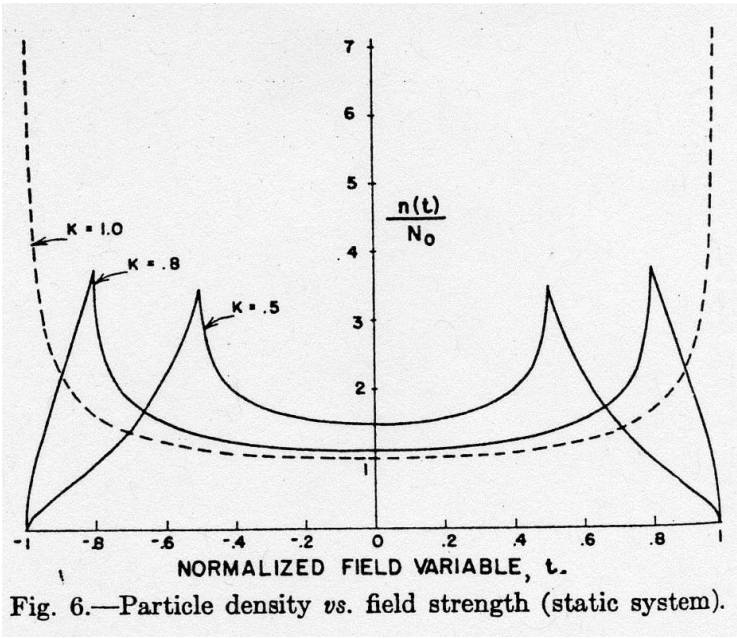

Fig. 6.—Particle density *vs.* field strength (static system).

Zimmerman and Foster J. Phys. Chem. 61,282 (1957)

P. Diehl et. al. Mol. Cryst. Liq. Cryst. 87, 319 (1982)

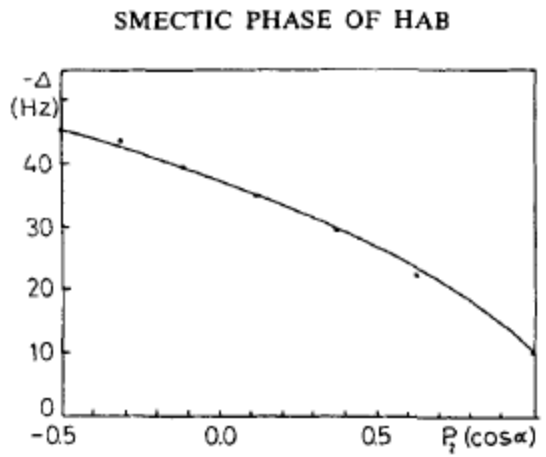

FIGURE 2 The water line splitting, $-\Delta$, as a function of $P_2(\cos\alpha)$. The solid c was calculated from Eq. (9). (●) are experimental points with errors ±1 Hz.

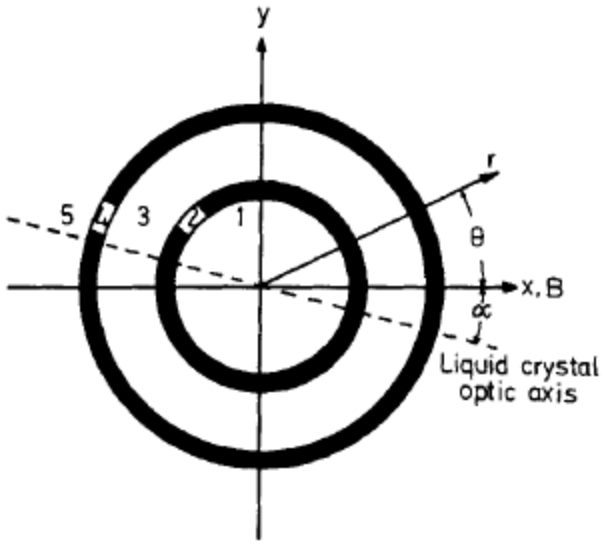

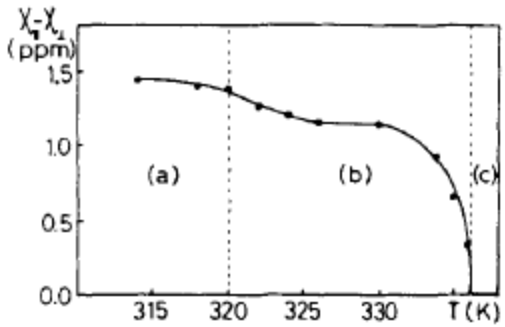

FIGURE 4 Anisotropy of diamagnetic susceptibility, $\chi_{\parallel} - \chi_{\perp}$, of HAB at various temperatures. (a) Smectic, (b) nematic, and (c) isotropic phase.

H. Cho et. al. JMR 88,198 (2009)

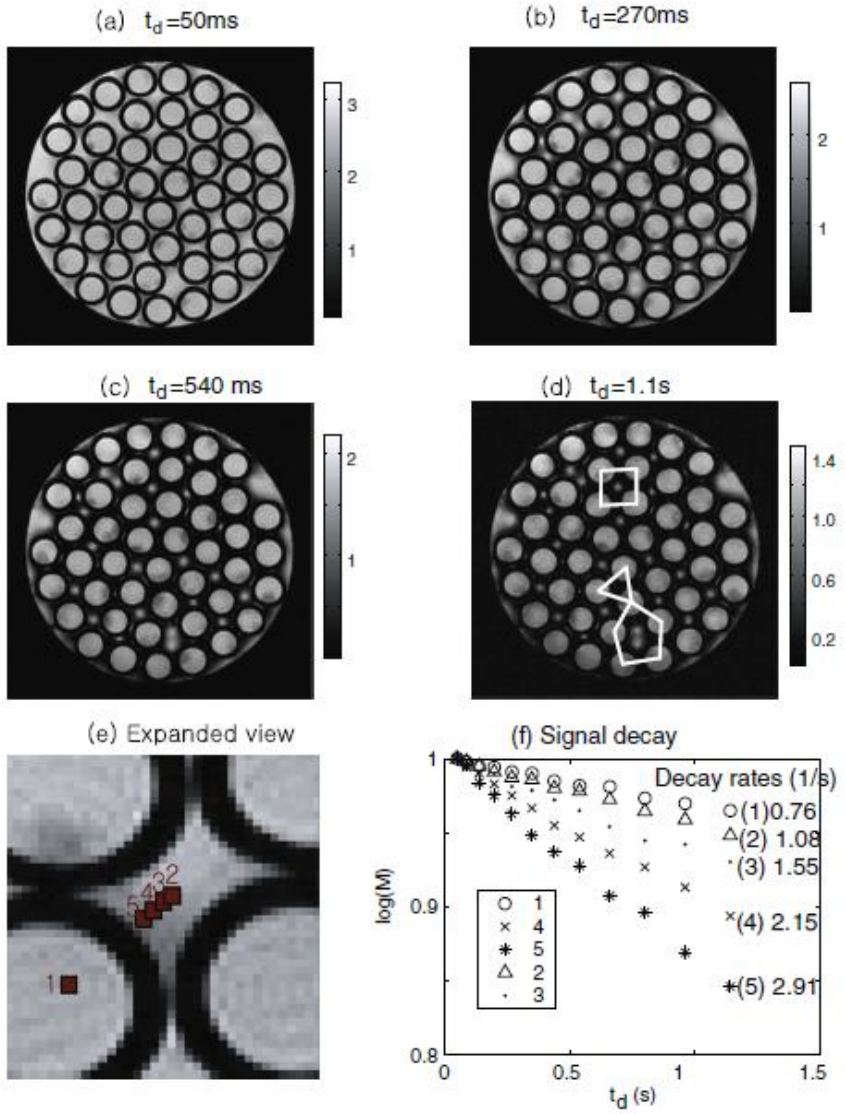

Fig. 2. Axial images with different diffusion times (t_d: 0.05 s (a), 0.27 s (b), 0.54 s (c) and 1.1 s (d)) show the spatially varying decay profiles across the pores. Several local packing geometries are highlighted in (d). (e) Shows a close-up of (a) and (f) plots the signal decay at the individual voxels denoted in (e).

Solid State NMR Example Chemical Shift Tensors for Biphenyl

Spherical Single Crystal

Detailed Analysis of Intermolecular contributions to the Chemical Shift Tensor

Frank Schonborn et. al.

JMR. 175, 52 (2005).

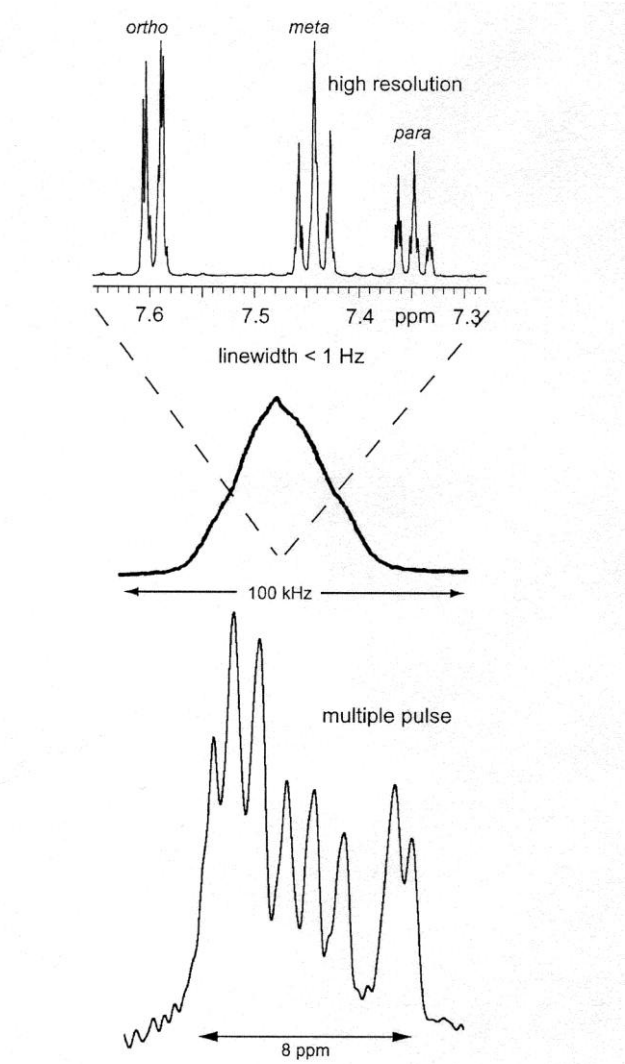

Fig. 3. A 500 MHz high resolution spectrum of biphenyl in $CDCl_3$, a solid-state wide line and a 270 MHz single-crystal multiple pulse spectrum. The width (FWHH) of the wide line spectrum is about 30 kHz or 110 ppm, the width of the resonances in the multiple pulse spectrum is about 0.7 ppm, i.e., line narrowing by a factor of 150 was achieved.

HR-MAS
Spinning Inhomogeneous Samples at the Magic Angle

- Isotropic Susceptibility
- Concentration Gradients
- Cell Suspensions
- Polymer Bead Synthesis, Seeds, etc.
- Rotate the Sample…….OR……
- Rotate the Magnetic Field!

Short Cylinder Field Profiles

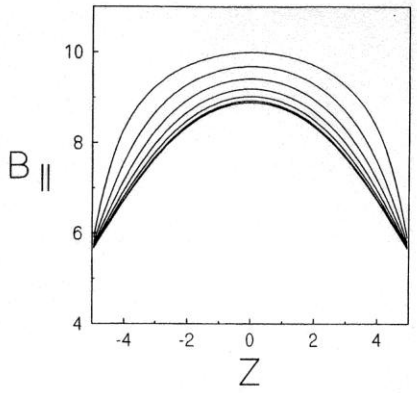

FIG. 2. Truncated demagnetization field for a cylinder oriented along the polarizing **B** field.

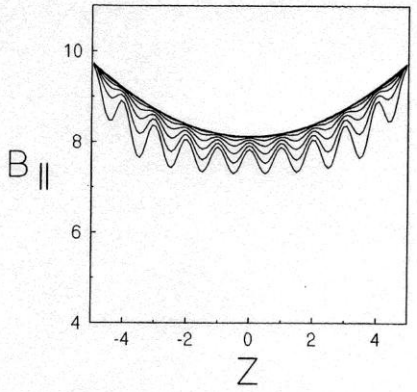

FIG. 4. Demagnetization field plots for a cylinder oriented perpendicular to the polarizing field.

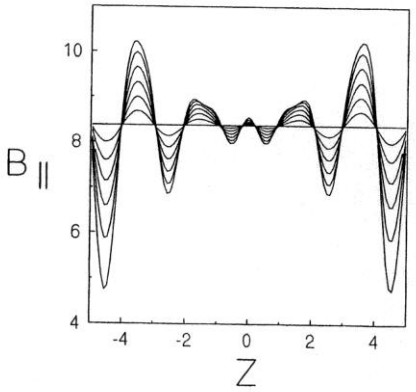

FIG. 3. Demagnetization field plots for a cylinder oriented at the magic angle with respect to the polarizing field.

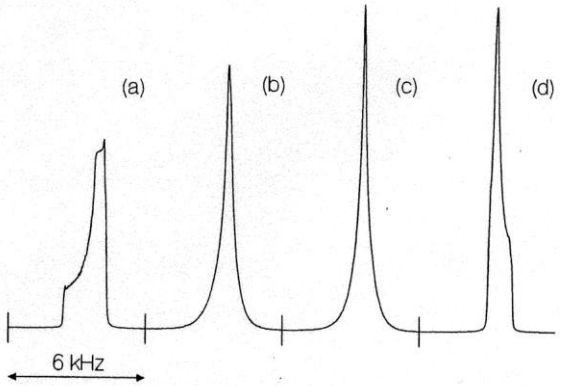

FIG. 5. Static lineshapes for a cylinder of water at 600 MHz as a function of cylinder orientation. (a) 0°, (b) 45°, (c) 55°, (d) 90°.

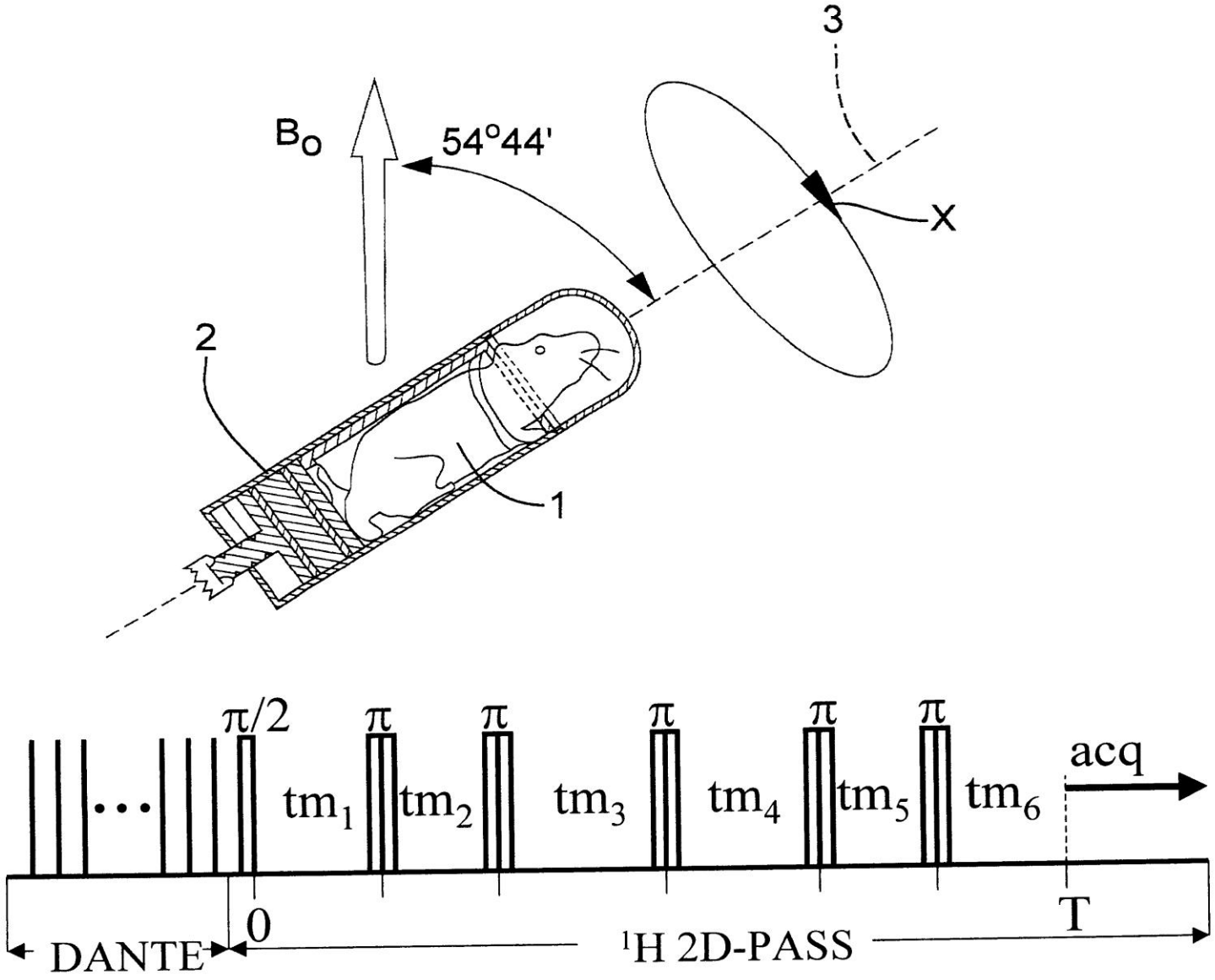

Robert Wind's proposal for Magic Angle Mouse Spinning

Varian Engineers attempt isotropic averaging of the speaker in 1998!
(I lasted about 10 seconds)

Magic Angle Rotating Magnetic Field (MARF)
Schlueter and Budinger
Dimitris Sakellariou, et. al.

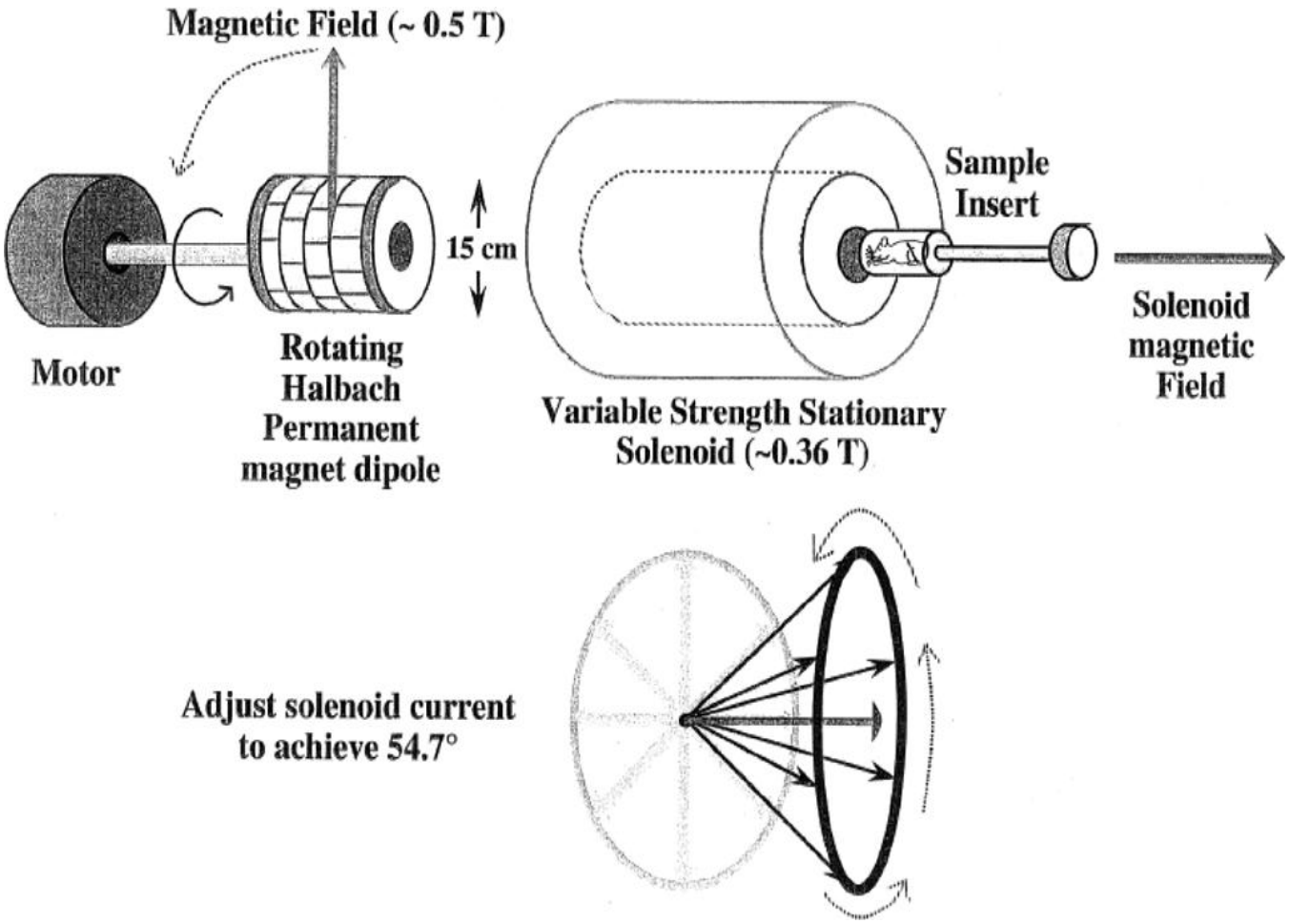

Rather than Rotating the Sample, One could Rotate the Magnet!

A Difficult Shimming Problem in MRI

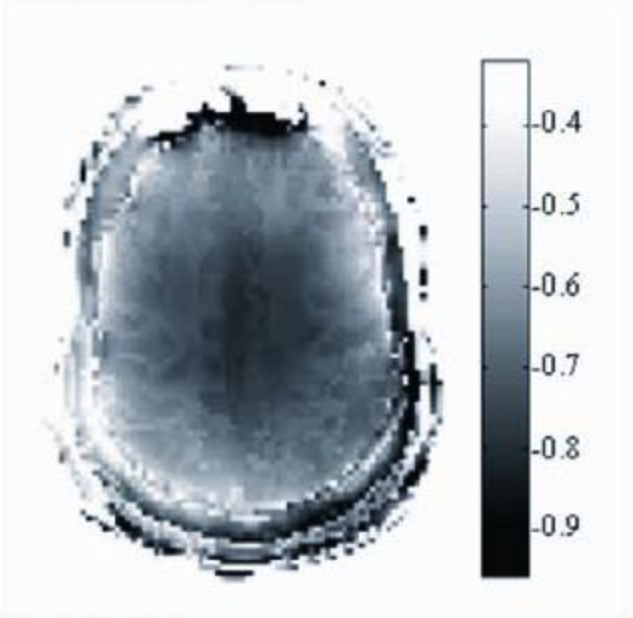

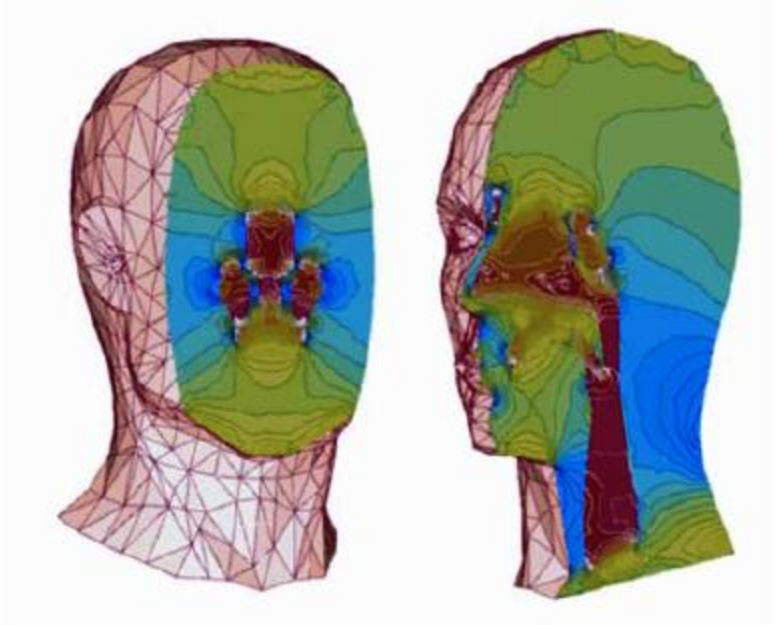

Qing X. Yang, Michael B. Smith, and Jianli Wang
The Pensylvania State University
College of Medicine, Hershey

MAGNETIC SUSCEPTIBILITY TOMOGRAPHY: A NEW MODALITY FOR THREE-DIMENSIONAL BIOMEDICAL IMAGING

I.M. THOMAS, N.G. SEPULVEDA, and J.P. WIKSWO, Jr.,

Department of Physics and Astronomy, Vanderbilt University,
Box 1807, Station B, Nashville TN 37235.

ABSTRACT

We have developed an algorithm that computes the three-dimensional magnetic susceptibility distribution inside a body from external magnetic measurements. In order to find the correct solution, it is generally necessary to collect data under various relative orientations of the applied field, the sample and the measurement locations. We show by simulation that the algorithm performs well with both high-precision and rounded data, provided that measurements are made in several different planes relative to the sample.

INTRODUCTION AND MAGNETIC THEORY

Biomedical imaging utilizes many different modalities of tomography [1]. In this paper, we discuss magnetic susceptibility tomography [2], which images the three-dimensional magnetic susceptibility distribution in a body from external measurements of the perturbation imposed upon an applied magnetic field. This technique could greatly improve the accuracy of quantitative liver iron susceptometry [3] and gastrointestinal transit studies utilizing magnetic tracers [4].

When a magnetic object is placed in an applied magnetic field $\mathbf{H}_a(\mathbf{r}')$, it modifies the field in a way that depends upon the distribution of magnetic susceptibility $\chi(\mathbf{r}')$. If the object is ferromagnetic, the magnetization of one region creates a secondary field (much stronger than the original applied field) which magnetizes adjacent regions, complicating the analysis. However, diamagnetic and paramagnetic materials (including biological tissues) satisfy the Born approximation, whereby the magnetization of any region is too weak to affect an adjacent one. Under this condition, the magnetic field $\mathbf{B}(\mathbf{r})$ measured near an object of volume v' is given by

$$\mathbf{B}(\mathbf{r}) = \frac{\mu_o}{4\pi}\int_{v'}\left\{\frac{3\chi(\mathbf{r}')\mathbf{H}_a(\mathbf{r}')\cdot(\mathbf{r}-\mathbf{r}')}{|\mathbf{r}-\mathbf{r}'|^5}(\mathbf{r}-\mathbf{r}') - \frac{\chi(\mathbf{r}')\mathbf{H}_a(\mathbf{r}')}{|\mathbf{r}-\mathbf{r}'|^3}\right\}dv'. \quad (1)$$

If the object is discretized into m elements ($0 \le i \le m$) each of volume v_i', small enough that the susceptibility within it may be assumed to be constant, the jth external field measurement ($0 \le j \le n$) may be written as

$$\mathbf{B}(\mathbf{r}_j) = \sum_{i=1}^{m}\mathbf{G}(\mathbf{r}_j,\mathbf{r}_i',\mathbf{H}_a(\mathbf{r}_i'))\chi(\mathbf{r}_i')v_i', \quad (2)$$

where the vector Green's function is given by

$$\mathbf{G}(\mathbf{r}_j,\mathbf{r}_i',\mathbf{H}_a(\mathbf{r}_i')) = \frac{\mu_o}{4\pi}\left\{\frac{3\mathbf{H}_a(\mathbf{r}_i')\cdot(\mathbf{r}_j-\mathbf{r}_i')}{|\mathbf{r}_j-\mathbf{r}_i'|^5}(\mathbf{r}_j-\mathbf{r}_i') - \frac{\mathbf{H}_a(\mathbf{r}_i')}{|\mathbf{r}_j-\mathbf{r}_i'|^3}\right\}. \quad (3)$$

In matrix notation, the field measurements may be written as the n elements of column matrix $\mathcal{B}$ and the Green's functions as the $(n \times m)$ matrix $\mathcal{G}$ so that the magnetic susceptibility of each of the m source elements will be given by the column matrix $\mathcal{X}$, in

$$\mathcal{B} = \mathcal{G}\mathcal{X}. \quad (4)$$

To solve this equation for $\mathcal{X}$, we can make the system overdetermined ($n > m$) and use a least-squares technique. We must also take steps to avoid $\mathcal{G}$ becoming ill-conditioned and this can be achieved by varying the relative geometries of the applied field, sample and measurement locations. Three strategies were considered:

1. Vary the direction of the applied field and keep the sample and the measurement locations fixed.
2. Vary the orientation of the sample and keep the measurement locations and the applied field fixed.
3. Vary the measurement locations and keep the applied field and the sample fixed.

We developed an algorithm that solves Equation 4 by singular value decomposition, and used it, with simulated data, to investigate each of these strategies. As shown in Figure 1a, the sample was a sixty-four-element cube, in which ten randomly-selected elements had been assigned $\chi = +2.5 \times 10^{-5}$ (SI), while the remainder had $\chi = +2.0 \times 10^{-5}$ (SI). Using a uniform applied field, the forward problem (Equation 1) was solved many times, yielding simulated high-resolution magnetometer data that were presented to the algorithm. To simulate experimental noise, the data were rounded to five significant figures in some calculations, while high-precision data, correct to about one part in 10^9, were used for the others.

Here is a very early Publication on "susceptibility imaging". Currently this is pursued via the use of Fourier Transforms. However, the inversion instabilities still plague the method.

The Fourier Transform Solution

R. Salomir et.al. Concepts in Magnetic Resonance 19B,26(2003).

J.P. Marques, R. Bowtell , Concepts 25B,65 (2004).

G. Deville et.al. Phys. Rev. B19,5666 (1979).

Applications to MRI: Susceptibility Weighted Imaging (SWI)

Y.N. Cheng et. al. Phys. Med. Biol. 54, 1169 (2009)

K.M. Koch et. al. Phys. Med. Biol. 51, 6381 (2006)

K. Shumueli et. al. MRM. 62, 1510 (2009)

There are some truly torturous derivations of the method in the literature. Here is a more direct approach.

$$\Phi_m = -\nabla \cdot \int d^3r' \frac{\mathbf{M}(\mathbf{r}')}{|\mathbf{r}-\mathbf{r}'|} \qquad \mathbf{H} = -\nabla \Phi_m$$

$$\mathbf{H} = \int d^3r' \left\{ \frac{3\mathbf{M}(\mathbf{r}')\cdot(\mathbf{r}-\mathbf{r}')}{|\mathbf{r}-\mathbf{r}'|^5}(\mathbf{r}-\mathbf{r}') - \frac{\mathbf{M}(\mathbf{r}')}{|\mathbf{r}-\mathbf{r}'|^3} \right\} \quad (\star)$$

Whoa!

If we work it out for $\mathbf{B}$ we recover

$$\mathbf{B}(\mathbf{r}) = 4\pi \mathbf{M}(\mathbf{r}) + \mathbf{H}$$

OK, this is just a sum of a bunch of Dipoles

$$\Phi_m = -\nabla \cdot \int d\underset{\sim}{r}' \frac{\underset{\sim}{M}(\underset{\sim}{r}')}{|\underset{\sim}{r}-\underset{\sim}{r}'|}$$

$$\frac{1}{|\underset{\sim}{r}-\underset{\sim}{r}'|} = \frac{1}{2\pi^2} \int d^3\underset{\sim}{k} \, \frac{1}{k^2} \, e^{i\underset{\sim}{k}\cdot(\underset{\sim}{r}-\underset{\sim}{r}')}$$

$$\hat{F}(\underset{\sim}{k}) = \int d^3\underset{\sim}{r} \; F(\underset{\sim}{r}) \, e^{-i\underset{\sim}{k}\cdot\underset{\sim}{r}}$$

$$\therefore \quad \hat{H}_{\perp N}(\underset{\sim}{k}) = 4\pi \left(\frac{1}{3} - \frac{k_z^2}{k^2} \right) \hat{x}(k) \, H_0$$

Much Easier than starting from (★)

Here is a recent effort on the use of the Fourier Inversion

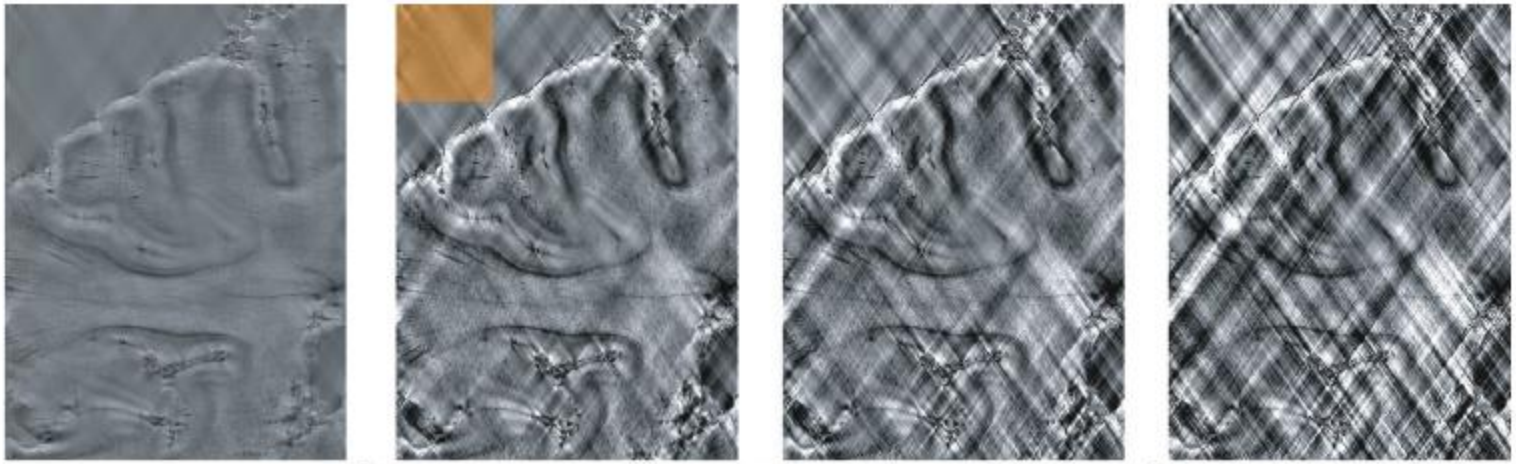

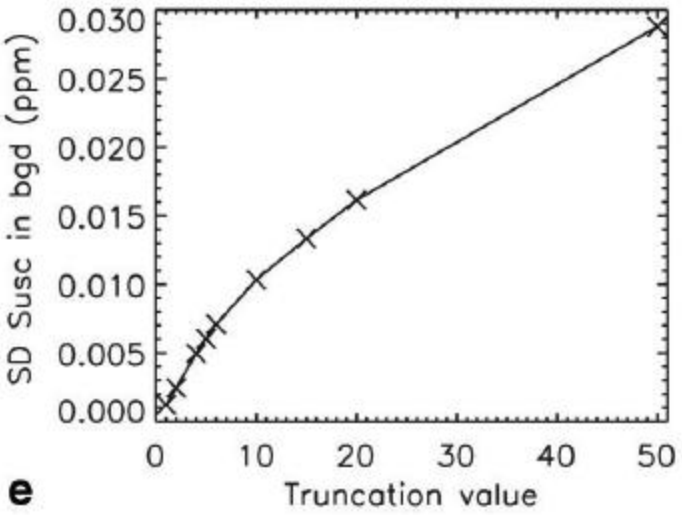

FIG. 4. The effect of truncation value on susceptibility maps. Susceptibility maps of a single slice of fixed human brain tissue shown in Fig. 3. The calculations were carried out with different *t* values for *F* in Eq. 2, i.e., 1 **(a)**, 5 **(b)**, 10 **(c)**, and 20 **(d)**. All the images are scaled between ± 0.04 ppm (40×10^{-9}). A graph of the SD of the susceptibility in the background region shown by the orange box in **(b)** against *t* is shown in **(e)**.

Although the method suffers from numerical instabilities, it appears promising for getting at local variations in susceptibility.

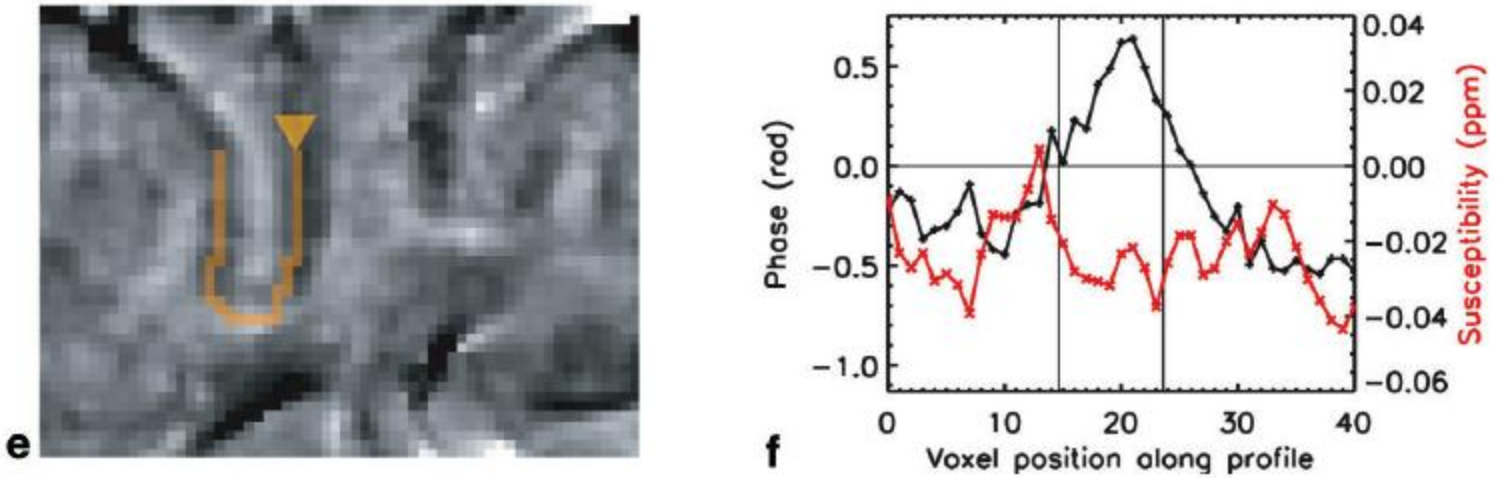

FIG. 5. Susceptibility maps in an occipital region of the human brain in vivo. One full coronal slice of the magnitude image is shown **(a)**, with a box outlining the region in which the susceptibility was calculated. The boxed region is zoomed, and its magnitude **(b)** residual phase ($\pm$ 5 Hz) **(c)** and calculated susceptibility ($\pm 50 \times 10^{-9}$) **(d)** are shown. The dashed tracings outline a band near the border between the gray and white matter, which is highlighted by the profile (in orange in **e**) on a zoomed region of **(c)**. The phase (black, from **c**) and susceptibility (red, from **d**) values along the profile **(e)** are plotted **(f)**, with voxel zero at the arrowhead. The left-hand phase axis in (f) is scaled such that any phase is equivalent to the phase that would arise inside a cylinder, parallel to B_0, with susceptibility equal to that shown on the right-hand axis. The vertical lines in **(f)** show the points at which the profile changed direction with respect to B_0.

A Dedication

I want to dedicate this talk to my undergraduate adviser , Paul L. Corio, pictured on the right with the speaker in 1972. Some of you may be familiar with his classic book on high resolution NMR.